RESONANT ABSORPTION OF 58-keV GAMMAS BY TERBIUM VANADATE, TERBIUM HYDRIDE, AN. ERBIUM METAL

David W. Oram

A thesis

in the

Department of Physics

Presented in partial fulfillment of the requirements

for the degree of Master of Science at

Sir George Williams University

Montreal, Canada

SEPTEMBER, 1974

ACKNOWLEDGMENTS

The author is indebted to Professor S.K. Misra for proposing this research topic, as well as for his help, advice, and encouragement during the course of the research. He would like to thank G.R. Sharp, a fellow graduate student, for the many valuable hours of discussion and assistance which greatly aided in the completion of this thesis. He acknowledges the encouragement and understanding received from his wife, Beatrix, and is certainly thankful to her for her expert typing of this thesis.

Thanks are also due to Professor N. Eddy for his help, suggestions and the loan of his detector, to Dr. R.C. Sharma for the loan of his cryostat, and to J. Blaison, J. Loustou, and A. Christodoulopoulos of the machine shop, for their technical assistance.

This work was partially supported by Dr. Misra's NRC grant.

RESONANT ABSORPTION OF 58-keV GAMMAS BY TERBIUM VANADATE, TERBIUM HYDRIDE, AND TERBIUM METAL

David W. Oram

ABSTRACT

The measurements of linewidths and isomer shifts of absorption spectra of 58 keV gammas by Tb^{159} nuclei in terbium metal (Tb), terbium vanadate ($TbVO_4$) and terbium hydride (TbH_3) absorbed by transmission Mossbauer spectroscopy are reported. The source used was Dy^{159} in dysprosium oxide (Dy_2O_3) host, the 58 keV gamma rays being obtained in the decay of 58 keV Tb^{159m} daughter state of Tb^{159}. All absorbers gave unsplit absorption lines. The measured linewidths (full width at half maximum, fwhm), extrapolated to zero absorber thickness, were found to be 12.5 $\pm$ 0.05 cm/sec, 9.85 $\pm$ 0.05 cm/sec, and 15.6 $\pm$ 0.05 cm/sec for the Tb metal, $TbVO_4$ and TbH_3 absorbers respectively, the isomer shifts being 1.2 $\pm$ 0.05 cm/sec, 0.79 $\pm$ 0.05 cm/sec, and 0.15 $\pm$ 0.05 cm/sec for the Tb metal, $TbVO_4$ and TbH_3 absorbers respectively. Using the

linewidth (extrapolated to zero absorber thickness) obtained for the Tb metal absorber, the lifetime of Tb^{159m} 58 keV was estimated to be $(5.66 \pm 0.01) \times 10^{-11}$ seconds. By the method of linewidth dependence on absorber thickness, the Debye-Waller factor for Tb metal was calculated to be 22.1%. Using this value, the Debye temperature was estimated to be $226^{\circ}K$.

TABLE OF CONTENTS

I. INTRODUCTION AND DISCUSSION OF BASIC IDEAS

The subject of this thesis is an experimental study of the absorption of the 58-keV gamma rays coming from Dy^{159} by terbium metal, terbium vanadate ($TbVO_4$) and terbium hydride (TbH_3). The motivation being ultimately the study by Mössbauer effect of the phase transition that takes place in $TbVO_4$ at about 33^oK by Dr. Misra's research group. As the Debye-Waller factor for the emission and absorption of gamma radiation by terbium is negligible at room temperature (i.e. f=0.3% at 300^oK), it was necessary to perform all of the experiments at a reduced temperature in order to increase the recoilless fraction (i.e. f=23% at 77^oK and f=39% at 0^oK).

Since atomic resonance radiation depends essentially on the existence of quantized energy levels and since such levels also exist within the nucleus, the possibility of observing nuclear resonance fluorescence was obvious, and an unsuccessful search was started by Kuhn[1] in 1929. Although it seemed that the problems in atomic and nuclear resonance were very similar, there existed marked differences which rendered nuclear experiments much more difficult.

It was not until 1950 that Moon[2] first overcame many of these difficulties and first observed nuclear resonance fluorescence and it was not until 1958 that R.L. Mössbauer[3] discovered the recoilless emission and absorption of gamma rays.

The phenomenon of the emission or absorption of a gamma ray photon without loss of energy due to the recoil of the nucleus and without thermal broadening is known as the Mössbauer Effect. In brief, under suitable conditions, the entire crystal in which a Mössbauer emitter or absorber is imbedded, rather than the single nucleus undergoing the transition, participates in the sharing of the momentum received during the transition of a gamma ray photon. Since the mass of the crystal is many times larger than that of the nucleus, the energy lost to recoil is greatly reduced. Because of the quantization of phonons (lattice vibrations) in a crystal, quantum mechanics predicts a finite possibility that the lattice does not take up any recoil energy and the entire energy of the nuclear transition goes into the gamma ray photon. This produces a gamma ray of natural width and Doppler broadening disappears.

Mössbauer applied Lamb's[4] theoretical work on the capture of slow neutrons in crystals to the analogous problem of the resonance absorption of gamma radiation.

His calculations resulted in equation 1,

$$P(n_s, n_s) \approx \exp\left\{\sum \frac{\left[-(2n_s+1)a_s^2(\hbar k)^2\right]}{2M\hbar w_s}\right. \tag{1}$$

which gives the probability that the lattice state remains unchanged after the emission of a gamma ray, i.e. for the occurrence of the Mössbauer effect. (This equation is based upon the assumption that the forces between the atoms are harmonic). In this equation, n_s is the occupation number of phonons for mode s, w_s is the harmonic oscillator angular frequency for the s^{th} mode, the factor $(\hbar k)^2/2M\hbar w_s$ is the ratio of the free recoil energy to the energy of the s^{th} mode and a_s is the coefficient which appears in an expansion of the co-ordinate of the centre of mass of the emitting nucleus in terms of the normal modes of the lattice.

Resonance experiments with gamma rays are usually performed by either measuring the scattered intensity or by determining the attenuation of a beam due to resonance absorption. The cross sections for these two processes, for an incident gamma ray of energy, E, and wavelength, $2\pi\lambda$ have been calculated[5] to be:

$$\sigma_{scatt}(E) = \sigma_o - \frac{\Gamma_\gamma^2}{4(E-E_T)^2 + \Gamma^2} \qquad (2)$$

$$\sigma_{abs}(E) = \sigma_o \frac{\Gamma\Gamma_\gamma}{4(E-E_T)^2 + \Gamma^2} \qquad (3)$$

The two above equation (2 and 3) apply in the case of ideally thin absorbers.

In these equations, Γ is the total width of the absorption line, Γ_γ , its gamma ray width and σ_o , the maximum resonance cross section, given by:

$$\sigma_o = \frac{2I_B + 1}{2I_A + 1} 2\pi\lambda^2 \qquad (4)$$

where I_A is the spin of the ground state, A, and I_B is the spin of the excited state, B.

Scattering and absorption cross sections given by equation 2 and 3 show a characteristic energy dependence of the form:

$$I_E = \frac{\Gamma}{2\pi}\left(\frac{1}{(E-E_\gamma)^2 + (\Gamma/2)^2}\right) \qquad (5)$$

which is normalized to:

$$\int_0^\infty I(E)\,dE = 1 \qquad (6)$$

This distribution is said to show a Breit-Wigner or Lorentzian shape and is sketched in Fig. 1. The parameter Γ, gives the full width at half maximum.

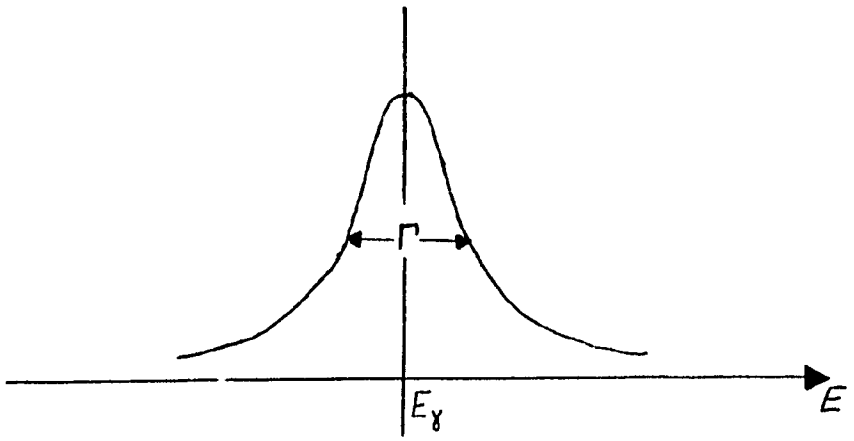

Fig. 1 The Lorentzian energy distribution of the source recoilless radiation

The absorption curve in an actual experiment displays a line width just twice that of the natural line width of a decaying nuclear state. The factor of two arises

because the observed absorption is the result of folding an emission spectrum together with an absorption spectrum, each of which has a width Γ.[6]

The Mössbauer effect provides a means of measuring radiation frequencies with extreme accuracy. It could register changes in the energies of nuclear transitions with a resolving ability $\Gamma/E = 10^{-12} - 10^{-15}$ eV. It became possible for the first time to study the hyperfine structure of nuclear transitions, as well as the influence of electric, magnetic and gravitational fields on the energy of gamma quanta. The non-displaced and non-broadened Mössbauer resonance line has become the basis of gamma ray spectroscopy.

Since its discovery, Mössbauer spectroscopy has become a tool exploited not only by nuclear and solid state physicists, but by physical and inorganic chemists, biologists, geologists, and many others in the solution of a wide range of scientific problems.

I.1 DEBYE-WALLER FACTOR

For the case of the Debye model of a solid, the fraction, f, of gamma rays emitted or absorbed without energy loss was calculated by Mössbauer. In a Debye solid, there exist a continuum of oscillator frequencies ranging from zero to a maximum frequency, obeying a distribution function. This calculation performed by Mössbauer[7] leads to equation 7,

$$f = e^{-2W} \tag{7}$$

where $w = 3\frac{R}{k\theta_D}\left[\frac{1}{4} + \left(\frac{T}{\theta_D}\right)^2 \int_0^{\theta/T} \frac{x\,dx}{e^{x-1}}\right]$

and R is the recoil energy of the emitting atom, k is Boltzmann's constant, θ_D is the Debye temperature and T is the temperature of the emitting atom in absolute degrees. It must be noted that this result is only valid if the concept of Debye temperature is applicable. In many instances, even for crystals consisting of only one kind of atom, the Debye theory cannot be used. The Debye-Waller factor was originally put forth to describe the scattering of X-rays without loss of energy to the lattice. The analogous quantity in the Mössbauer effect is sometimes called the Lamb-Mössbauer factor.

I.2 ISOMER SHIFT

Isomer shift is also sometimes called chemical shift. The nucleus interacts with the surrounding electronic charges. The energy of interaction can be found by considering a uniformly charged spherical nucleus imbedded in its electron charge cloud. A change in the s-electron density will result in an altered Coulombic interaction which manifests itself as a shift of nuclear levels.

In heavy elements, the addition of one or more neutrons alters the nuclear radius. This change in turn shifts the atomic energy levels. A change in the radius can occur even without a change in nucleon number when the nucleus goes from one state to another, i.e., when it decays from an isomeric state to the ground state. The corresponding shift in energy in called an isomeric shift. A change in nuclear radius which shifts the atomic energy level, will also affect the nuclear levels by the same amount. If the charge density in the source and absorber are unequal, the amount of energy given up in compressing the nucleus in the source will not be equal to the amount of energy gained in expanding the nucleus in the absorber. Thus if the electrostatic spring constants in the source and absorber are unequal, the

energy of the Mössbauer resonance line will be shifted.

Three requirements are necessary for the observation of a nuclear isomeric shift:

(i) The two nuclear states involved must have different charge distributions,

(ii) There must be electronic wave functions (usually from the s-electrons) which overlap appreciably with the nuclear wave functions,

(iii) These wave functions must be sensitive to external (chemical) changes.

The shift relative to some standard substance, which manifests itself in a Mössbauer spectrum as a displacement of the resonance peak from the zero velocity position (see Fig. 2) is[3]

$$I.S. = \frac{2}{5}\pi Z e^2 \left(R_{ex}^2 - R_{gd}^2\right)\left(|\Psi(0)|_a^2 - |\Psi(0)|_s^2\right)$$

$$= \frac{4}{5}\pi Z e^2 R^2 \left(\frac{\delta R}{R}\right)\left(|\Psi(0)|_a^2 - |\Psi(0)|_s^2\right) \qquad (9)$$

where R_{ex} and R_{gd} are the root mean square radii of the excited and ground states and $|\Psi(0)|^2$ is the non-relativistic s-electron density at the centre of the nucleus. $|\Psi(0)|^2$ can be computed from a hydrogen-like wave function

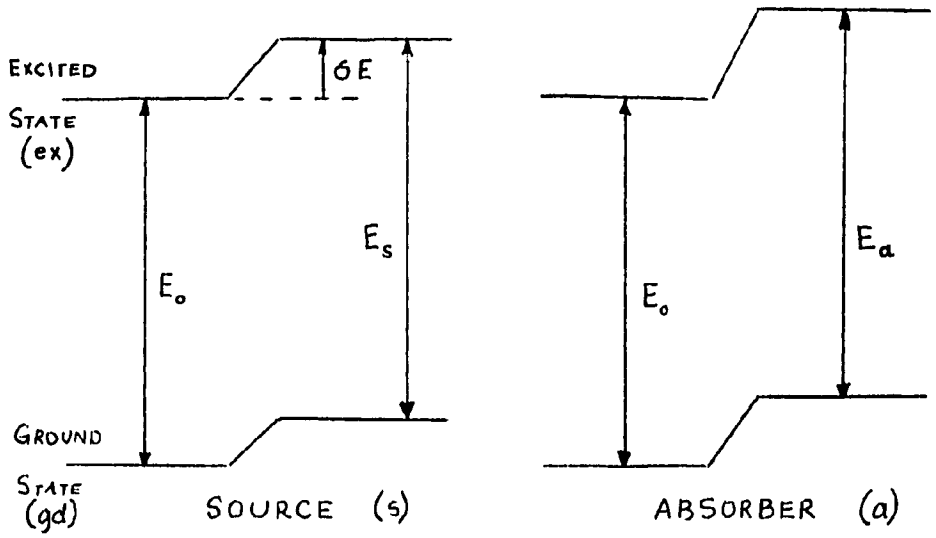

$$\delta E = \frac{2\pi}{5} Ze^2 \left|\Psi(0)\right|^2 R^2 \quad \text{(RELATIVE TO POINT NUCLEUS)}$$

$$E_s = E_o + \frac{2\pi}{5} Ze^2 \left|\Psi_s(0)\right|^2 \left[R_{ex}^2 - R_{gd}^2\right]$$

$$E_a = E_o + \frac{2\pi}{5} Ze^2 \left|\Psi_a(0)\right|^2 \left[R_{ex}^2 - R_{gd}^2\right]$$

$$\text{ISOMER SHIFT} = E_a - E_s$$

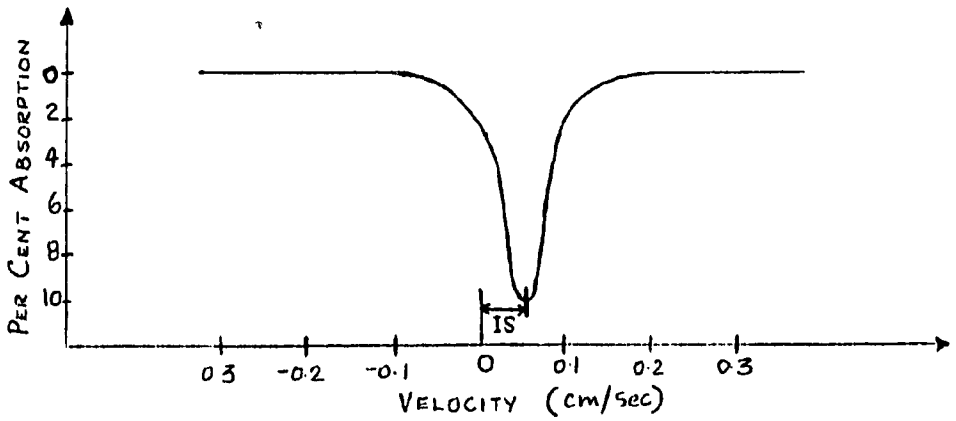

Fig. 2. Isomer Shift. The effect of the electric monopole interaction is to shift nuclear levels. The shifts are very small compared to the total energy of the gamma ray, $10^{-12} E_\gamma$.

or, more accurately, from the Fermi-Segré formula.[9] This equation consists of two factors, one which contains only a nuclear parameter $\delta R/R$ and the second containing the electronic charge density at the nucleus, which is an atomic or chemical parameter.

The experimental measurement of the isomer shift will give only the products of these two parameters and if one is to know both parameters, one of them must be calculated from theoretical considerations.

I.3 DETERMINATION OF RECOILLESS FRACTION

A. LINE WIDTH METHOD

In the usual transmission experiment, the counting rate of photons behind an absorber is measured as a function of velocity of the source relative to the absorber. In our case, we are concerned with a single line absorber illuminated by a single line source.

The most appropriate parameter for determining the recoilless fraction in the absorber is the full width at half maximum of the Mossbauer absorption peak.

The most complete theoretical expression derived

thus far is due to J. Heberle[10] and relates the experimental absorber linewidth W to the "apparent thickness", t, of the absorber.

$$W = 2\Gamma\left[1 + 0.1288t + (4.733\times10^{-3})t^2 - (9.21\times10^{-4})t^3 + (3.63\times10^{-5})t^4\right] \quad (10)$$

$$\text{and} \qquad t = n\sigma_0 f_a \quad (11)$$

where n is the number of active nuclei per cm^2; σ_0 is the maximum cross section; and f_a is the recoilless fraction. Equation 10 is applicable under the limits, $0 < t < 12$.

Visscher[11] has also derived two formulae similar to equation 10, but applicable only over smaller ranges of t values.

B. LINE WIDTH DEPENDENCE ON ABSORBER THICKNESS

A linear dependence of experimental line width on absorber thickness is given by:[12]

$$W = \Gamma_a + \Gamma_s + 0.27\, n\sigma_0 \Gamma f_a \quad (12)$$

$$\text{for } \frac{\Gamma}{\Gamma_a} n\sigma f_a < 5$$

where W is the experimental linewdith (fwhm), Γ is the natural linewidth, Γ_s and Γ_a are the linewidths of the source and absorber respectively. Thus a graph of W/Γ as a function of $n\sigma_o$ will be a straight line of slope $0.27\ f_a$. This gives a value of f which does not involve a knowledge of the other three unknowns. The intercept occurring at $n\sigma_o = 0$ gives a value of $\Gamma_a + \Gamma_s$.

C. AREA METHOD

Calculations for a Lorentzian shape Mössbauer spectrum of fwhm Γ_{exp} and peak dip p_{exp} lead to:[13]

$$AREA = \frac{\pi C}{2E_o}\left(\Gamma_{exp}\, p_{exp}\right) \tag{13}$$

with

$$p_{exp} = \frac{\Gamma_a}{\Gamma_{exp}}\left(f p(t)\right) = \frac{2\Gamma h(t)}{\Gamma_{exp}}\, f p(t) \tag{14}$$

where

$$p(t) = \left[1 - e^{-t/2}\, I_o(t/2)\right] \tag{15}$$

$$h(t) = (1 + 0.135\, t) \qquad 0 \le t \le 5$$
$$h(t) = (1 + 0.145\, t - 0.0025\, t^2) \qquad 4 \le t \le 10 \tag{16}$$

For small t:

$$0 \le t \le 5 \qquad p_{exp} = n\sigma_o \frac{\Gamma}{\Gamma_{exp}}\, f f' (1 - 0.24t + 0.04t^2) \tag{17}$$

For large t:

$$4 \leq t \leq 10 \qquad p_{exp} = 1.2 f \left(\frac{\Gamma'}{\Gamma_{exp}} + 0.20\, n\sigma_0 f' \frac{\Gamma}{\Gamma_{exp}} \right) \qquad (18)$$

where f is the fraction of photons emitted without recoil and f' is the fraction of photons absorbed without recoil.

If f' is known from a separate experiment, (eg. from a recoil-free Rayleigh scattering experiment), f can be deduced precisely from the above equations, even if the natural emission linewidth Γ' is not known precisely. Otherwise thin absorber experiments may determine ff' and t, but not f and f' separately unless Γ' is known, but one usually has enough information on f to deduce f' from the product ff'.

Another expression for $t < 6$ is given by Lang[14], where the absorption area integral is given by:

$$A = \frac{1}{2} f \Gamma \pi L(t) \qquad (19)$$

where Γ is the natural linewidth and the function L(t) is given by:

$$L(t) = \sum_{p=1}^{\infty} \frac{(-1)^{p+1} (2p-3)!!\, t^p}{p!\,(2p-2)!!} \qquad (20)$$

The function L(t) for values of t from zero to 30 have been computed and are given by Hafemeister.[15]

D. COMPARISON METHOD

There is a fourth method for the determination of the recoilless fraction, but this method yields somewhat distorted values, especially when dealing with thick absorbers.

The magnitude of the maximum absorption, $\eta(0)$, has been calculated[16] to be:

$$\eta(0) = f\left[1-\exp\left\{-\frac{1}{2}t\right\} I_0\left(\frac{1}{2}it\right)\right] \qquad (21)$$

where $I_0\left(\frac{1}{2}it\right)$ is a zero order Bessel function with imaginary argument, t.

In a Mössbauer experiment, it is possible to determine directly the quantity $\left[N_\infty - N_v\right]/\left[N_\infty - N_b\right]$, where N_∞ and N_v are the rates of count of the number of gamma quanta in the absorber at very high speeds (i.e. resonance absorption effect absent) and at velocity, v, respectively and N_b is the rate of count of background gamma quanta which is independent of the velocity. After determining the quantity N_b from auxilliary experiments and eliminating it from $\left\{N_\infty - N_v \middle| N_\infty - N_b\right\}$ it can be shown[17] that f and f' may

be determined from:

$$\frac{N_\infty - N_r}{N_\infty} = f\left[1 - \exp\left\{\frac{-t}{2}\right\} I_o\left(\frac{it}{2}\right)\right] \qquad (22)$$

II. DETAILS OF APPARATUS USED

A brief description of some of the important components of the system shown in Fig. 3 will now be described.

II.1 DETECTOR

As in any experiment involving the detection of radiation, the choice of the most appropriate detector was of vital concern. The energy of gamma rays and X-rays encountered in Mössbauer effect studies varies from about 3-4 keV to 200 keV and therefore different types of nuclear radiation counters are needed to detect radiations of different energies. The requirement for energy discrimination to distinguish Mössbauer radiation from gamma rays or X-rays with nearly the same energy coupled with the need for maximum efficiency, dictates the nature of the detector.

A proportional counter was used at first, but it gave poor resolution and very low efficiency because it was being used to detect radiation whose energy was higher than the useful energy range of the counter.

Below 40 keV, the gas-filled proportional counter gives

good resolution but low efficiency (which specifies the fraction of the flux incident on the counter that is detected) and reliability as compared to the scintillation type of crystal. The scintillation-crystal type of detector is used in detecting gamma rays of energy from 50 to 100 keV. A silicon detector was used that gave much greater resolution and an improved efficiency. The efficiency of the particular detector available, however, was still too low in view of the fact that the percentage of counts going into the resonance dips was in the vicinity of 1%. Finally a lithium-drifted germanium detector was employed. The use of this detector further increased both resolution and count rate. It consists of a PIN (p type, intrinsic, n type) semiconductor made of lithium doped germanium. The intrinsic region is normally non-conducting, but when the gamma radiation ionizes the lithium doped region, conduction takes place and a pulse is produced. The pulse height is proportional to the gamma ray energy.

The detector used was a Nuclear Diodes (Ge-Li) detector with a 4% efficiency relative to a 3 x 3 NaI crystal, using a source of Co^{60} at a distance of 25 cm. from the detector.

From Fig. 4, the resolution of the detector was:

$$\text{Resolution} = \frac{\Delta E}{E} = 5.5\ \%$$

where ΔE is the half width of the 58.0 keV X-ray peak and E is the corresponding energy of the peak, both values being expressed in terms of channel number.

II.2 MÖSSBAUER VELOCITY-DRIVE CONTROL UNIT

The control unit is a solid state electronic unit which accepts a square wave signal from the address register of a multichannel analyzer. It contains shaper and integrator, difference amplifier and d.c. power amplifier required to drive the transducer. The velocity control unit is used to produce a voltage which is applied to the transducer, causing a velocity of the transducer varying linearly with time in a parabolic motion with constant acceleration. The displacement as a function of time, consists of segments of parabolas of positive and negative acceleration. The displacement, and the corresponding velocity and acceleration of the parabolic motion, as a function of time, are shown in Fig. 5.

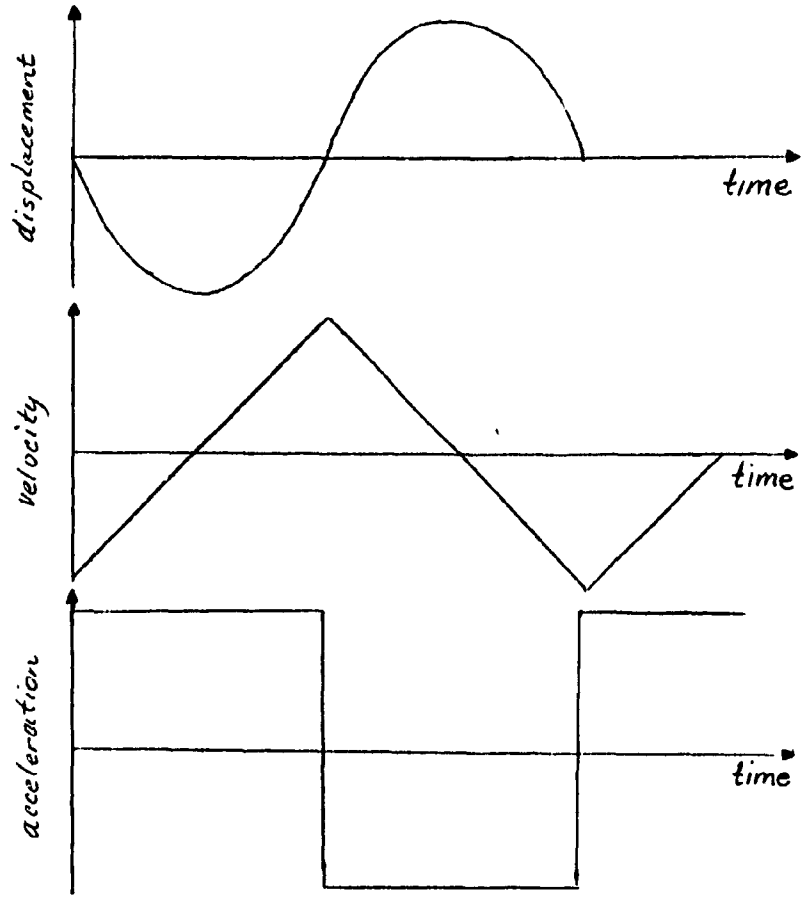

Fig. 5 The displacement velocity and acceleration of the source as a function of time.

II.3 TRANSDUCER

The Doppler motion between source and absorber necessary to produce a Mössbauer spectrum is provided by an electromechanical drive system which is controlled by a servo amplifier. The amplifier is fed with a reference voltage waveform which repeats itself exactly. The actual

transducer embodies two coils, one of which produces a voltage proportional to the actual velocity of the shaft. The servo amplifier compares this signal to the reference waveform and applies corrections to the drive coil to minimize any differences. In this way, the centre shaft, which is rigidly connected to the source, executes an accurate periodic motion.

The transducer housing is equipped with vacuum flanges to which end bells are fastened when the system is used in conjunction with the cryoflask for low temperature operation.

The velocity signal of the transducer used was a symmetrical double ramp (i.e. triangular). It thus scanned half of the spectrum with a constant acceleration and scanned the other half of the spectrum with a constant deceleration of the same magnitude as that of the acceleration in the first half, producing a double (mirror image) spectrum. The transducer was equipped with two pairs of springs, one pair allowing speeds in the range of 0-15 cm/sec, the other permitting speeds in the range of 0-60 cm/sec. The operating frequency range of the transducer was 15-50 cps and the system linearity as measured was found better than 1% over 95% of the half period of the velocity waveform.

II.4 SINGLE CHANNEL ANALYZER

Differential discriminators, often called single-channel analyzers, are circuits producing a normalized digital output pulse for every input pulse, the amplitude of which satisfies the condition $V_c < V_{in} < V_c + \Delta V_c$. Pulses with amplitudes lower than V_c or higher than $V_c + \Delta V_c$ are suppressed. In the experiments performed, the single-channel analyzer was used to "pick out" the 58.0 keV peak in the spectrum of Dy^{159}. This was done by placing the window of the analyzer in the region of the voltage pulses that had heights associated with the 58.0 keV gammas. Thus only those pulses were permitted to pass through the analyzer. The analyzer used was the Hewlett Packard, model 5583A, single-channel analyzer.

II.5 MULTICHANNEL ANALYZER

The analyzer system used had the capability of three basic types of measurements. These measurements were: a) pulse-height analysis, b) multichannel scaling, and c) averaging. The analyzer system consisted of two units. These units were the ND 180F analog-to-digital converter (F unit) and the ND 180 memory unit (M unit). The primary function of the F unit was to digitalize analog information

so it could be used by the M unit. Other functions of the F unit were amplification of low level signal pulses, selective acceptance of input signals on an amplitude basis, and generation of "live time" signals during periods when the system was not busy with the processing of input signals. The M unit was basically a digital computer. The primary function of this unit was to totalize and store data supplied by the F unit or some other external source. It also performed the additional functions of digital-to-analog conversion of stored data to external translating devices and master system control.

II.6 LOW TEMPERATURE TEXAS INSTRUMENTS CRYOSTAT

Since the recoilless fraction is negligible at room temperature, it was decided to perform the experiment with both the source and absorber at liquid nitrogen temperature, necessitating the use of a cryoflask.

The cryoflask used was a vacuum insulated dewar with a vapour cooled radiation shield. (See Fig. 6). It provided for operational and laboratory use of liquid helium, hydrogen, neon and nitrogen as refrigerants. The cryoflask was a triple jacketed one with an outer jacket called the "case", the middle jacket termed the "radiation shield" and the inner jacket was the "flask". The entire

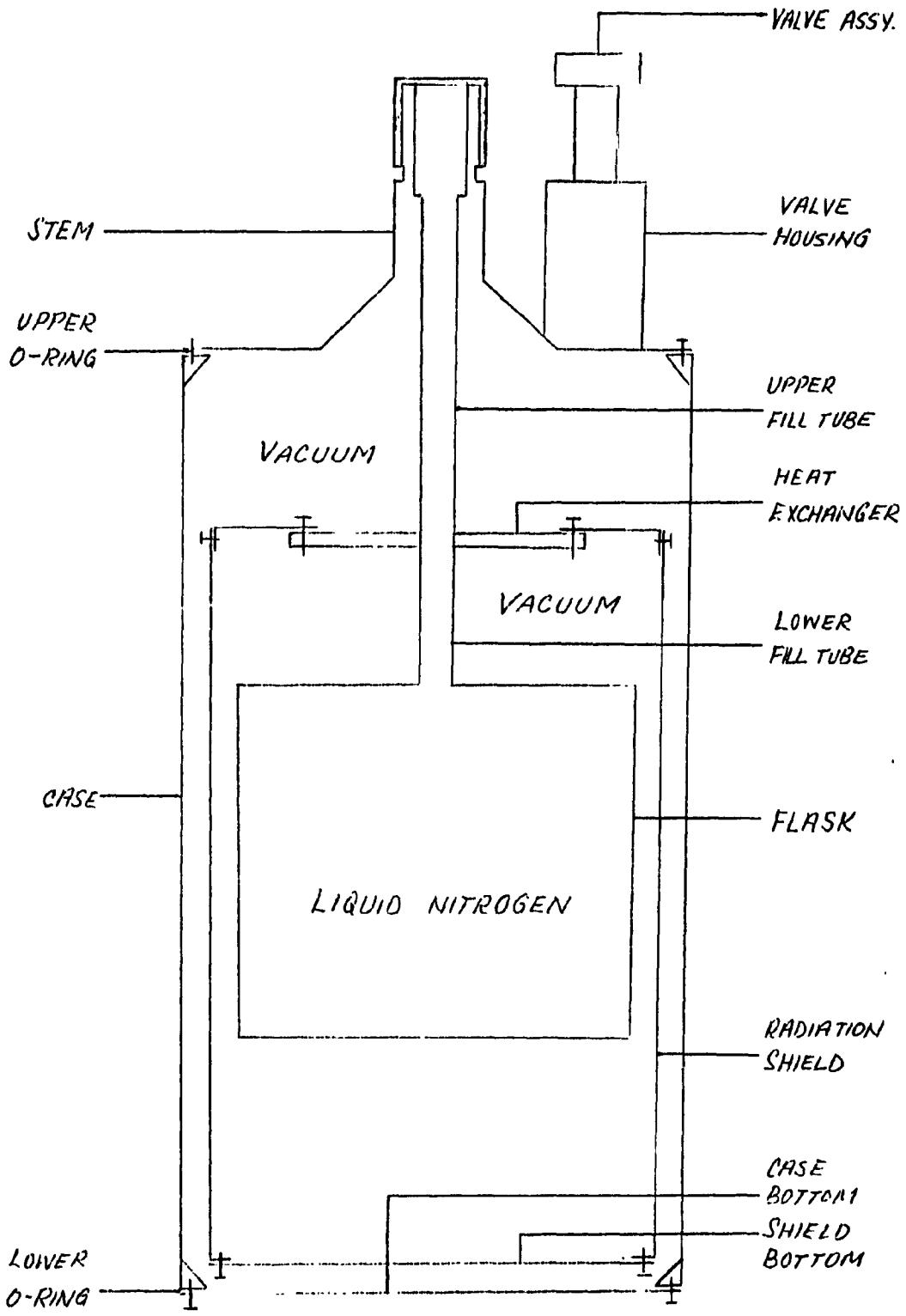

Fig. 6 Low Temperature Cryostat

space between the flask and the case was evacuated. The radiation shield and flask were supported from the "stem" of the case by the upper and lower fill tubes. The fill tubes were joined by the heat exchanger.

The cryoflask was designed to hold the source attached to the transducer under vacuum and at the temperature near that of the refrigerant. It could also be used to cool the absorber at the same time. There were connectors on the cryoflask designed for a vacuum gauge and temperature measuring.

II.7 SOURCE

The source used was Dy^{159} (15 mC strength) in Dy_2O_3. Dy^{159} decays with a half life of 144 days to form Tb^{159}. Tb^{159m} decays by gamma emission (58.0 keV, $+5/2 \rightarrow +3/2$) to Tb^{159}, which is 100% naturally abundant. The beta decay of Dy^{159} proceeds by electron capture. The pulse-height analysis of the source spectrum is shown in Fig. 4 and the decay scheme is shown in Fig. 7.

It was prepared by New England Nuclear Corporation by taking approximately 13 mC of $DyCl_3$ and precipitating it with NH_4OH. The precipitate was dried at 120°C and the DyO_3 powder was cast in Lucite by hot high pressure

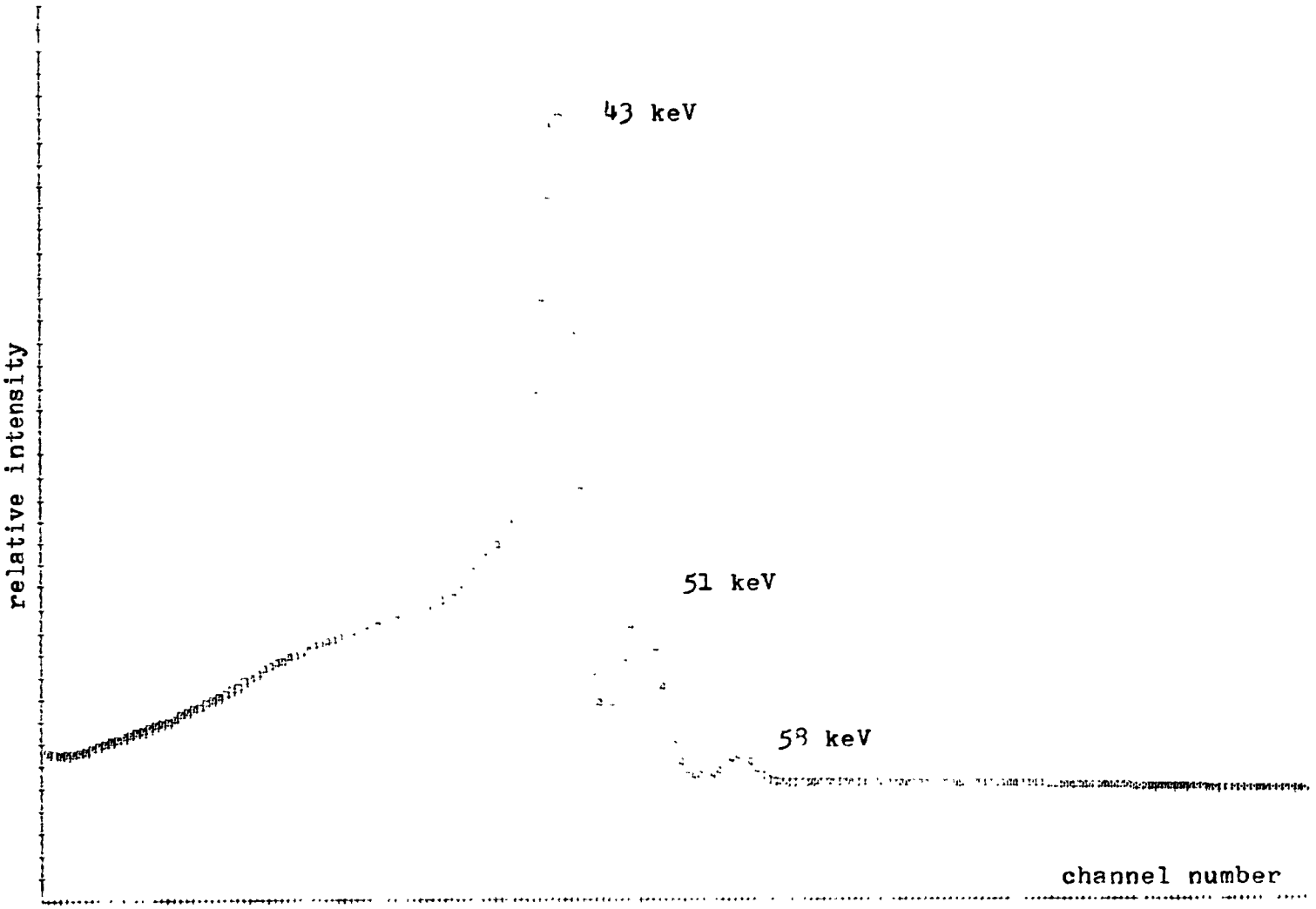

Fig. 4 Pulse Height Analysis Spectrum of Dy^{159}.

casting. The dimensions of the source were 5 mm of active area in a 12 mm plastic mount. The isotope specific activity was 2.30 mCi/mg.

A source foil of Co^{57} in copper was used for velocity calibration. Its strength was estimated to be under 2 mC.

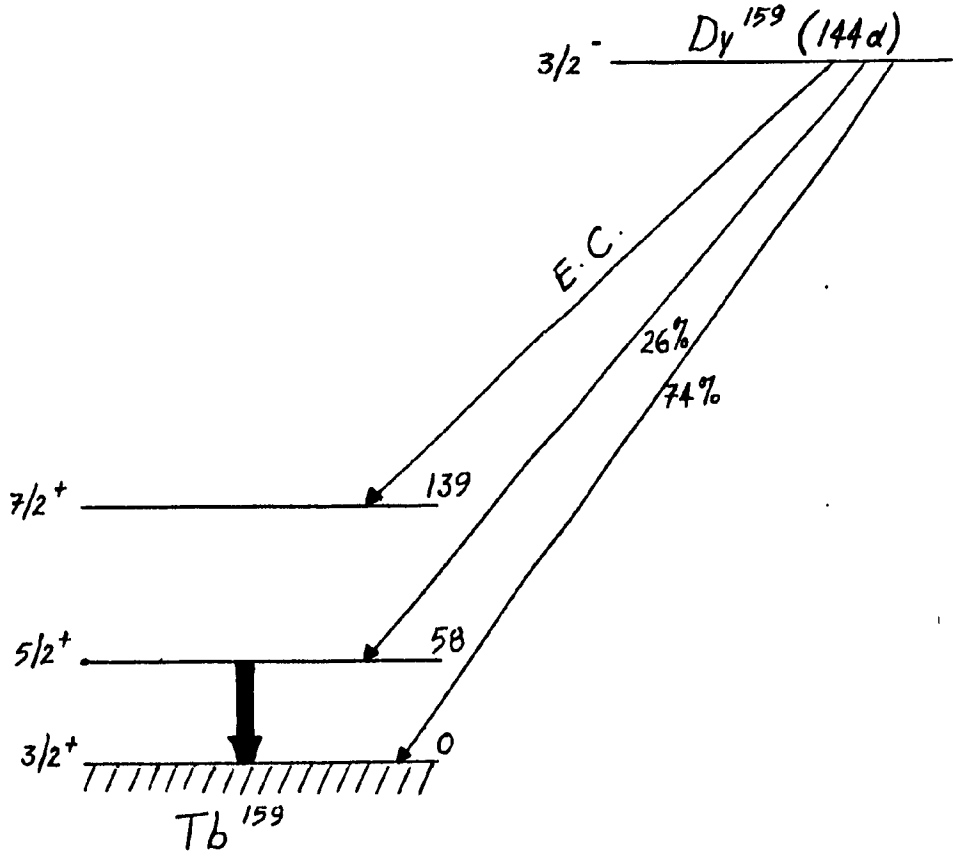

Fig. 7 Decay Scheme of Dy^{159}.
(not to scale)

II.8 ABSORBERS

Four different kinds of absorbers were used in the course of the Mössbauer experiments. The first was a solid disk (2.6 cm in diameter and 0.3 cm in thickness) of sodium nitroprusside (N.P. = $Na_2 Fe(CN_5)NO \cdot 2H_2O$, sodium pentacyanonitrosyl ferrate (II)) used in the velocity calibration of the transducer. The other three were $TbVO_4$, TbH_3 and Tb metal which were the absorbers under study.

$TbVO_4$ was purchased from New England Nuclear Corporation. In the experiments performed, three thicknesses of $TbVO_4$ were used.

Tb metal was purchased, in granular form, from Alfa Inorganics and three different absorbers of this were made.

Terbium hydride was also purchased from Alfa Inorganics and only one absorber was made from it. (For a list of the thicknesses and weights of all absorbers used, refer to Table 1).

The absorbers made from the samples under study were all in powder or granular form, except for the third absorber of terbium metal, which was a metal foil of area 6.55 cm^2 and thickness 5/1000 in.

The method used to prepare those absorbers made from

powdered or granular samples was to manually impact the sample into the centre of a thin hollow disk of lucite of thickness 1.5 mm and radius 1.9 mm. No adhesive was used in the absorber preparation, as it was essential that all of the powder could be recovered. This method of absorber preparation is probably the greatest single factor contributing to errors in linewidths and line positions.

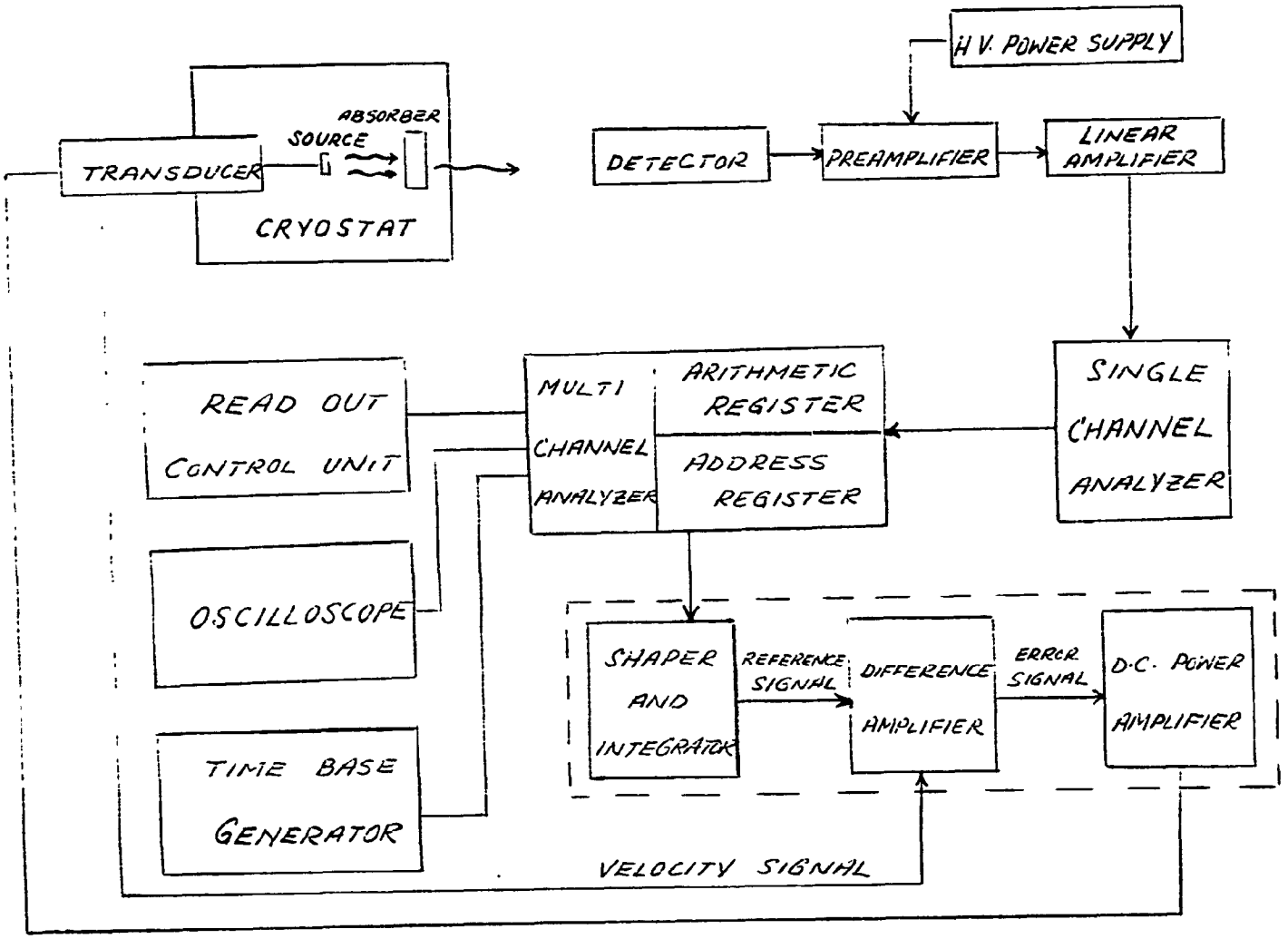

Fig. 3 Schematic arrangement for a Mössbauer experiment

III. FUNCTIONING AND USAGE OF APPARATUS AND METHOD OF ANALYSIS

The method describing how the apparatus was used to record the data of interest and the techniques involved will now be discussed.

III.1. RECORDING OF A MÖSSBAUER SPECTRUM

The recoil-free gamma ray energy of a typical Mössbauer transition is so precisely defined that its Heisenberg width corresponds to the energy change produced by an applied Doppler velocity of the order of 1 mm/sec. There is, therefore, an easily realizable relative velocity between source and absorber at which the gamma ray energy from the source will precisely match the nuclear energy level gap in the absorber and resonant absorption will be at a maximum. For a source and absorber which are chemically identical, this relative velocity will be zero. Application of an additional velocity increment will lower the resonant overlap and decrease the absorption. If a sufficiently large relative velocity is maintained, resonance will be completely destroyed. A Mössbauer spectrum comprises a series of measurements at different velocities (i.e., energies) across the resonant region.

Gamma rays coming from a transition are partly absorbed and partly transmitted. The transmitted ones pass into the detector and are transformed into an electric pulse proportional in height to the energy of the gamma ray. This analog pulse is then amplified. Part of the pulse spectrum is selected by a single channel analyzer which produces unit pulses. A multichannel analyzer counts each pulse from the single channel analyzer in the channel which is open at that moment. (Fig. 3).

In these experiments, a rapid scanning through the whole velocity range and subsequent numerous repetitions of this scan enabled one to accumulate all the data for the individual velocities essentially simultaneously. This was accomplished by operating the multichannel analyzer in the multiscaler mode and thus deriving a constant increment of velocity for each channel. The requirements of a linear velocity scale coupled with that of a flat non-absorption spectrum means that equal lengths of time must be spent in equal velocity increments. This is equivalent to requiring constant acceleration, which implies a motion that is parabolic in time. The multichannel analyzer is therefore used as a time analyzer (i.e. it is allowed to step at a clock controlled rate through its channels). Synchronism between the transducer and the analyzer is maintained by using the analyzer itself as the wave form generator.

Synchronously with the repetitious scan through the channel address scaler, a binary flip flop in the analyzer address system will switch from one memory half to the other, thus producing a square wave signal. By shaping this square wave with an operational amplifier, a very accurate square wave can be obtained, which can be modified by integration with additional operational amplifiers to produce triangular and parabolic waves, which can, in turn, be combined with an additional operational amplifier. The signal produced is the reference signal so as to impart a velocity to the transducer. (Each channel will correspond to certain velocity interval). The difference between reference and pick up produces an err. signal. (Fig. 8).

III.2 VELOCITY CALIBRATION

For the precision needed in Mössbauer experiments, an accurate measurement of the absolute velocity of the drive is required. This is one of the more important and difficult aspects of Mössbauer spectroscopy. The method most commonly used (because of its inexpensiveness) is to utilize the spectrum of a compound wh... has been calibrated as a reference. This is the method that was used and the compound in this case was sodium nitroprusside, which was irradiated by a Co^{57} source. Unfortunately, no suitable

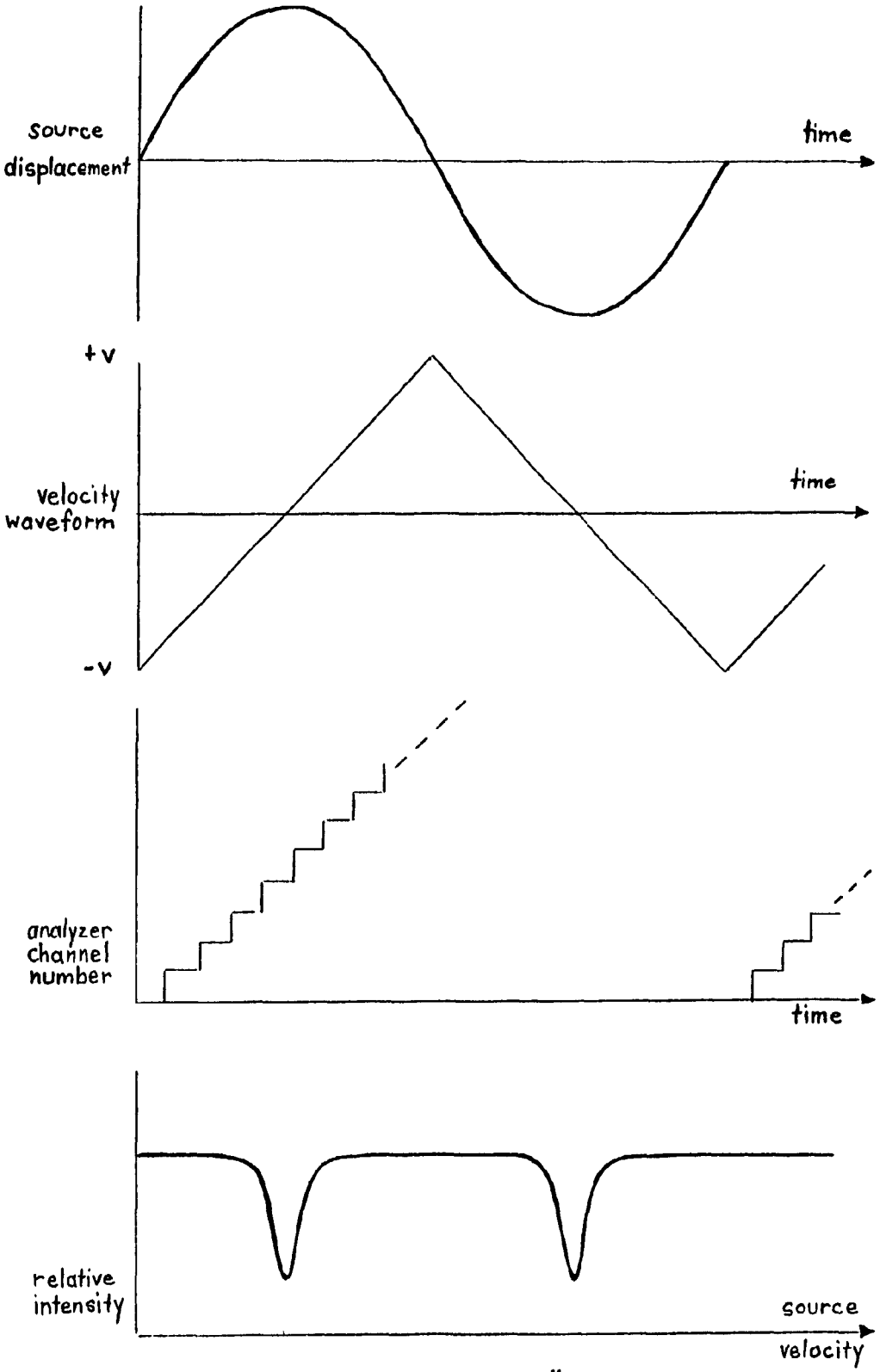

Fig. 3. RECORDING OF A MÖSSBAUER SPECTRUM

international standards or criteria have yet been decided upon. But sodium nitroprusside has often been used for this purpose because of the ease and preciseness for obtaining a spectrum with it.

The purpose of the calibration is to enable one to convert the channel number to absolute energy units. The spectrum of N.P. has only two peaks and the most accurate determination of the parameter of N.P.[18] gives the quadrupole splitting as 1.7048 $\pm$ 0.0025 mm/sec.

The procedure followed was to record the spectrum of N.P. using a Co^{57} source for some particular velocity setting on the spectrometer. The data from this spectrum was then run through a least squares fitting program which was used to fit the experimental data to a Lorentzian distribution. The separation between the two peaks obtained from the results of the curve fit were then compared to the known separation existing between them. That ratio, coupled with the knowledge that the maximum velocity occurred in the 128^{th} channel led immediately to the following relation existing between the absolute Doppler velocity (V) and the number of channels separating the peak positions (N):

$$V = \left(\frac{1.7048 \times 128}{N} \right) \text{ mm/sec}$$

This calculated value of the velocity was then compared with the original reading on the velocity control. The above procedure was repeated four times, each time for a different velocity setting. The final step was to plot a calibration curve of absolute velocity vs. velocity on velocity control dial. (Fig. 9).

The transducer speed used for all experiments was 24 cm/sec as read off the velocity control knob of the Mossbauer spectrometer. Using the value of the slope found in the previous graph, the absolute velocity of the transducer could be estimated. (It was reasonable to assume that a noticeable deviation between the observed and absolute velocities exist, considering the fact that in the course of the experiments, both the drive and pick-up coils of the transducer burnt out, and were replaced manually). The absolute velocity so calculated was determined to be equal to the observed reading times the slope = 24 cm/sec x 1.15 = 27.6 cm/sec.

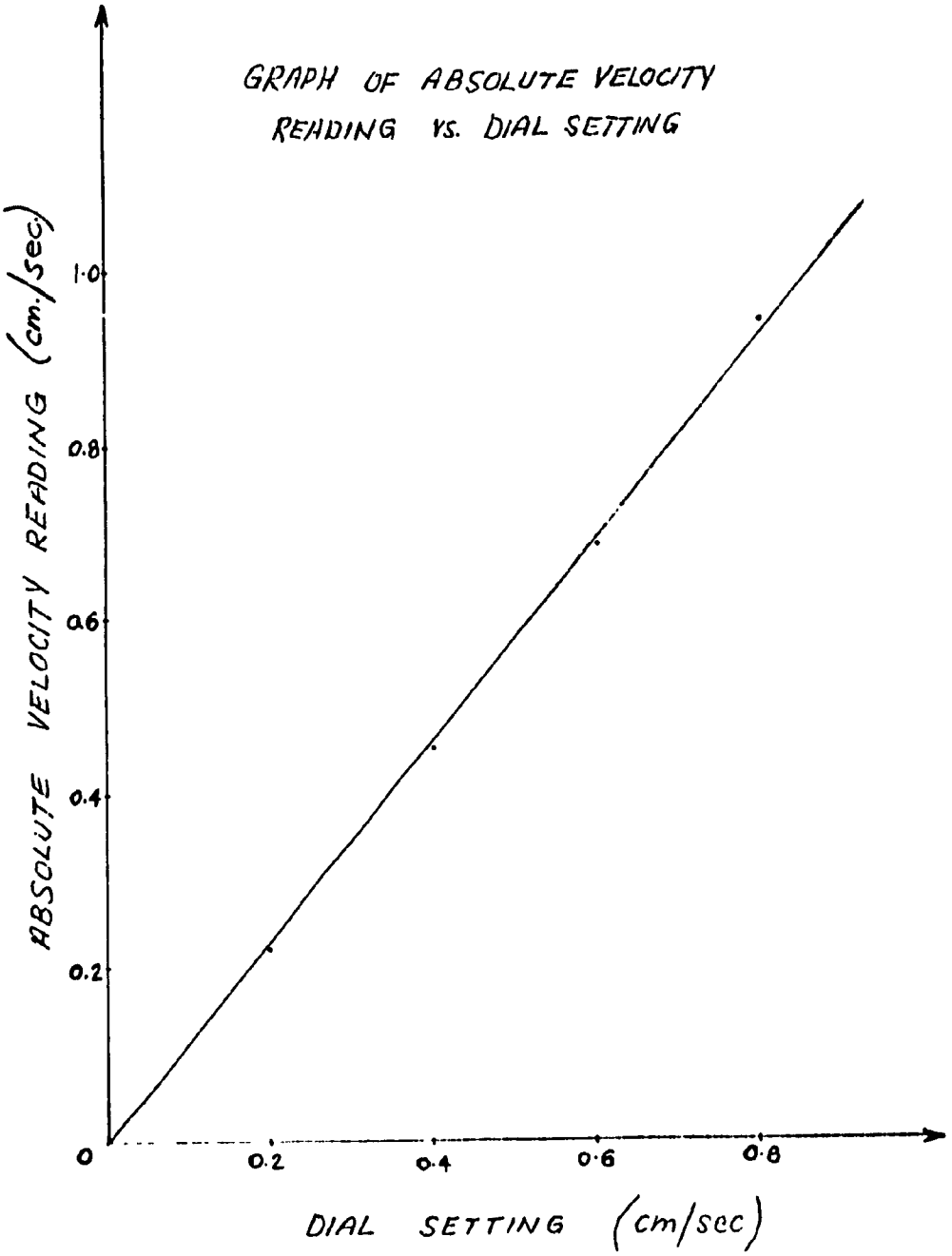

FIGURE 9 VELOCITY CALIBRATION CURVE

III.3 TEMPERATURE CALIBRATION AND CONTROL

All of the successful experiments performed were done so at reduced temperatures. The most common temperature used was that obtained by using liquid nitrogen as a refrigerant (77°K). This created the need to be able to measure accurately temperatures in the range of 0°K to 300°K.

Resistance thermometers (i.e. temperature sensors) were used to measure all temperatures and because of the large range in temperatures, both a platinum resistance thermometer and a germanium resistance thermometer were necessary, as each gives satisfactory performance only in certain temperature ranges. (Agreement between platinum and the absolute temperature scale is so close and well defined that it has been internationally agreed that it shall be taken as the Absolute Temperature Scale in the range -183°C to 660°C, provided that the thermometer is made of platinum that meets the appropriate specifications. Germanium resistors are used in the area of liquid helium temperatures, i.e. 4.2°K).

The temperature controller was an Artronix, model 5301. This instrument could control over a range of 1.0°K to 320°K, with six ranges for sensors with a positive temperature coefficient (i.e. platinum) and six ranges for sensors with

negative temperature coefficients (i.e. germanium), 40 ohms to 15K ohms. The temperature set control was a ten turn dial which provided continuous temperature settings throughout each range selected.

The resistance thermometers were calibrated by comparing their values to a previously calibrated set of platinum and germanium thermometers. Both calibrated and uncalibrated thermometers were placed in a cryostat and subjected to continuously decreasing temperatures and were joined in series to a constant current source. A calibration curve of resistance vs. temperature was available for the calibrated set of sensors. Then for a given temperature, the resistances of the set of uncalibrated sensors was obtained by using the constant current and voltage readings and thus a curve of resistance vs. temperature was obtained for the uncalibrated sensors also.

The dial on the temperature set control was calibrated using a standard resistance box and selecting the values of the resistance from the temperature vs. resistance curves for the platinum and germanium resistance thermometers. Each curve of temperature set vs. temperature was then fitted to a polynomial of maximum degree ten.

III.4 REMOVING ERRORS DUE TO THE SOLID ANGLE EFFECT

Since the Doppler energy shift is relative to the source and absorber only, it is independent of the frame of reference. For transmission experiments, it is usually more satisfactory mechanically to move the source. It is then much easier to change absorbers and to vary their temperature. The only major problem is that the source of the gamma rays and the detector are then not at rest relative to each other and the solid angle subtended by the source varies during the motion. (See Fig. 10). If the amplitude of the source motion is large, as it was in these experiments, a correction term should be applied. To further increase the error in these experiments, the source detector distance was minimal, in order to improve a very poor count rate. The shorter the source-detector distance is, the greater the variation of the solid angle that the detector sees. Fig. 11 shows the spectrum of $TbVO_4$ without any correction for the solid angle being applied. A large solid angle in the counting geometry thus introduces a distortion into the shape of the Mössbauer absorption line. This distortion can be minimized by maintaining an adequate separation between source and detector by collimation of the gamma ray beams.

The method derived to eliminate this distortion will now be discussed.

It was assumed that the observed spectrum was the superposition of two separate spectra. One of which was the Lorentzian curve showing a resonance peak and the second was a parabolic curve. By using the co-ordinates of points in the first quarter and last quarter of the observed spectrum, the form of the parabola was estimated. The estimated parabolic curve was then subtracted off the original data to yield ideally just the resonance spectrum.

The parabola that was estimated took the form:

$$y = \frac{(N-128)^2}{4p} + k + B \qquad (23)$$

where N is the channel number; P is the intensity difference between the vertex and the focus of the parabola; k is the value y takes when N = 128 channels and B is the background obtained by averaging the first ten and last ten channels of the observed spectrum.

Fig. 12 shows the same spectrum as Fig. 11, except the solid angle effect has been effectively eliminated.

10(a)

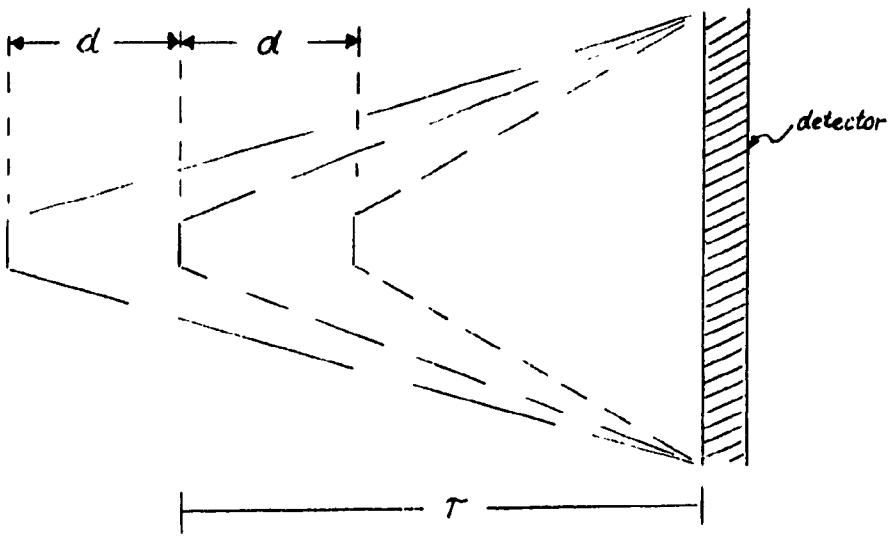

10(b)

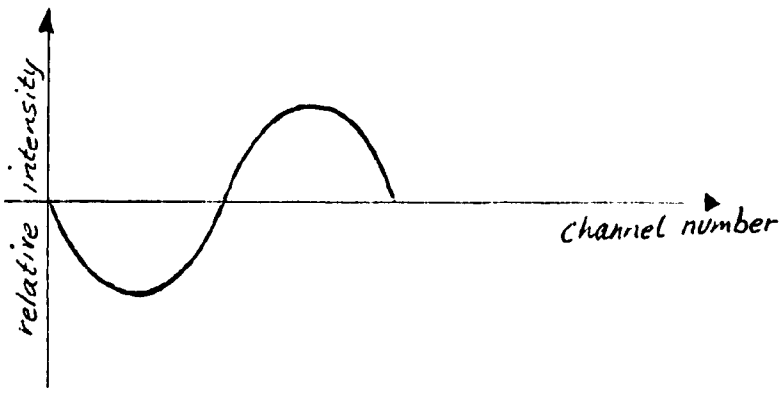

Fig. 10(a) shows how the movement of the source alters the solid angle of gamma rays as seen by the detector.

Fig. 10(b) shows how this altered solid angle influences a spectrum when no resonance is occurring.

N.B. The convention universally adopted is that a closing velocity between source and absorber (i.e. a higher energy) is defined as positive.

Fig. 11 Mössbauer Spectrum of $TbVO_4$ Before Removal of Solid Angle Effect.

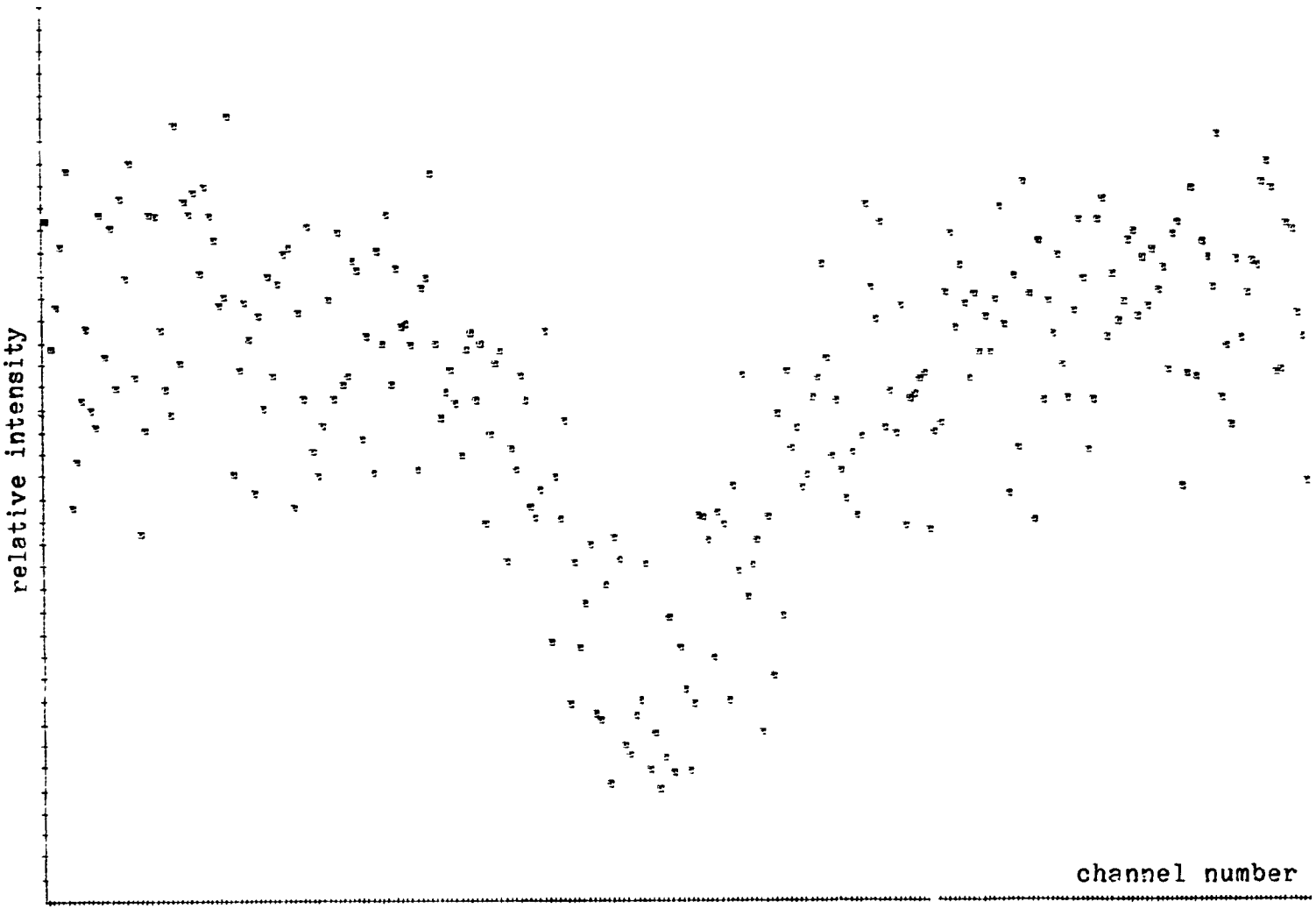

Fig. 12 Mössbauer Spectrum of $TbVO_4$ After Removal of Solid Angle Effect.

III.5 ANALYSIS OF DATA

In order to decide what particular values experimentally determined parameters shall take, it is necessary to find a statistically satisfactory method for extracting such values as the line position, line height and fwhm from the original experimental data. This problem is of particular importance in nuclear physics owing to the statistical nature of the decay process of radioactive nuclei.

Such a method, refered to as the "method of least squares" has been shown to obtain the most reliable possible information from a set of experimental observations and was the method used to analyze all data in these experiments.[19,20]

The principle of least squares can be stated as follows: The most probable value of a quantity is obtained from a set of measurements by choosing the value which minimizes the sum of the squares of the deviations of these measurements.

In our case, the best least squares fit was obtained for those parameter K which minimize the function defined by:

$$M\left(X_i^{exp}\right) = \sum_{i=1}^{256} \left(X_i^{exp} - X_i^{th}\right)^2 \Big/ \left(2\sigma_i^2\right) \qquad (24)$$

where X_i^{th} is the corresponding number of counts calculated from an estimation of the parameters fitted into the desired distribution function; X_i^{exp} is the measured number of counts recorded in the i^{th} channel; σ_i is the standard deviation of X_i^{exp}. For each individual channel, there is a unique Poisson distribution and the number of counts recorded in that channel is a random sample from it. The best estimate of the standard deviation of a sample drawn from a Poisson parent distribution is simply the square root of the mean. In our case, there was only one reading per channel and so it was necessary to use this as an estimate of the mean number of counts in this channel. So:

$$\sigma_i = \sqrt{X_i^{exp}} \tag{25}$$

The Mössbauer spectra obtained in these experiments were assumed to have a Lorentzian shape whose profile may be given by the function:

$$X_i(k_j) = X_i(A, X_j, \Gamma)$$

$$= B - \left(\frac{A}{1 + \left(\frac{X_i - X_j}{\Gamma} \right)^2} \right) \tag{26}$$

where B is the background and A is the amplitude of the peak located in channel $X_i = X_j$ with a full width at half maximum

of Γ.

It is important to note that it was assumed the data fitted well to a Lorentzian distribution. It was possible to determine how well the data fitted the distribution function by using the χ^2 test. The function χ^2 is defined as:

$$\chi^2 = \sum \frac{[Nf(n) - F(n)]^2}{Nf(n)} \qquad (27)$$

where n is an individual event; f(n) is the frequency of occurrence of event, n, from the sample; F(n) is the frequency of event n as predicted by the parent distribution; and N is the total number of trials. Now if the experimental data fits the parent distribution exactly $\chi^2 = 0$. But the larger χ^2 is, the more disagreement exists between the parent and sample distributions.

Now in order to minimize M(x), the following condition must be satisfied:

$$\frac{\partial M(x)}{\partial k_j} = 0 \qquad \text{with } j = 1, \quad 3M \qquad (28)$$

where 3M is the maximum number of parameters for a spectrum with M Lorentzian peaks. It would be sufficient if all the

eigen values of the second derivative matrix are positive. Equation 28 is never wholly satisfied, but $\Delta\left(\frac{\partial M(x)}{\partial k_j}\right)$ can be made as small as possible by adjusting a precision fitting parameter in the program.

Expanding $X_i(K_j)$ to the first order:

$$X_i\left(\vec{k}\right) = X_i\left(\vec{k}_o\right) + \Delta\vec{k} \cdot \nabla \vec{X}_i \Big|_{\vec{k}=\vec{k}_o} \tag{29}$$

with $\Delta\vec{k}=\vec{k}-\vec{k}_o$. Equation 24 then becomes:

$$M(x) = \sum_{i=1}^{N} \left(\frac{X_i^{exp} - X_i\left(\vec{k}_o\right) - \nabla\vec{X}_i \cdot \Delta\vec{k}\Big|_{\vec{k}=\vec{k}_o}}{2\, X_i^{exp}} \right)^2 \tag{30}$$

The solution $\Delta\vec{k}$ which minimizes M(x) is given by:

$$\Delta\vec{k} = -\alpha^{-1} \nabla\sqrt{M(x)} \tag{31}$$

where α is the second derivative matrix (or error matrix). An iteration process was then started that attempted to minimize M(x) by a proper choice of the parameters K_j. The minimum is achieved with $\Delta\vec{k} \rightarrow 0$. The results of each iteration and their convergence will show whether the input parameters and the line shape are of the proper choice.

A program called TRACEUR was used to plot by CALCOMP

the experimental Mössbauer spectrum together with the one resulting from the curve fitting. (The program was written by Dr. S.K. Misra of Sir George Williams University).

IV EXPERIMENTAL RESULTS AND THEIR INTERPRETATION

IV.1 DETERMINATION OF THE HALF-LIFE OF Tb^{159}

The inherent width of a gamma ray arises from the finite time (usually characterized by the half-life of the state) which the nucleus must spend in the excited state. This is clearly shown in Heisenberg's uncertainty relation:

$$\Delta E \cdot \Delta t \geq \hbar \tag{32}$$

The uncertainty in energy ΔE corresponds to the width of the nuclear state and appears also as the linewidth of the gamma ray, while the uncertainty in time corresponds to the mean life τ of the nuclear state. The ground state nuclear level has an infinite lifetime and has zero uncertainty in energy. So equation 32 may be written as:

$$\Gamma \tau \geq \hbar \tag{33}$$

The mean life is related to the half-life by the relation:

$$\tau = \ln 2 \times t_{\frac{1}{2}} \tag{34}$$

which makes it possible to rewrite equation 33 as:

$$\Gamma = \frac{0.693\,\hbar}{t_{1/2}} \tag{35}$$

Now Γ in the above expression is the natural linewidth, but it is known[6] that the observed experimental linewidth must be at the very least equal to Γ and will usually be larger than that. So:

$$\left[\frac{W}{2}\right] \geq \frac{0.693\,\hbar}{t_{1/2}} \tag{36}$$

where W is the experimentally determined linewidth. Solving equation 36 for $t_{\frac{1}{2}}$, the calculated value for the half-life of Tb^{159} (using the results obtained from Tb metal spectra), is 5.659×10^{-11} seconds.

IV.2 DETERMINATION OF THE RECOILLESS FRACTION

The method used to determine the recoilless fraction was the linewidth dependence on absorber thickness as outlined by O'Connor.[12] This method involves the graphical solution of the equation:

$$W = \left\{\Gamma_a + \Gamma_s\right\} + 0.27\, n\, \sigma_o\, f_a\, \Gamma \tag{37}$$

where: Γ_a is the absorber linewidth,

Γ_s is the source linewidth,

Γ is the natural linewidth,

n is the number of nuclei per square centimeter,

σ_o is the maximum resonance cross section,

f_a is the recoilless fraction of the absorber,

W is the experimental full width at half maximum.

If a graph of W/Γ vs. $n\sigma_o$ for different thicknesses of the same absorber is plotted, the result should be a straight line whose slope is equal to 0.27 f_a and whose x-intercept gives a value of $(\Gamma_a+\Gamma_s)$. The y-intercept should give a value of the experimental full width at half maximum extrapolated to zero thickness. The value of n was determined by the relation:

(38)

$$n = \left(\frac{\text{actual weight}}{\text{molecular weight}}\right) \times \left(\frac{\text{Avogadro's number}}{\text{cross sectional area of absorber}}\right)$$

The value of σ_o used was 9.827×10^{-20} cm.^{2} This value being obtained from the relation:

(39)

$$\sigma_o = 2.446 \times 10^{-15} \frac{1}{E_\gamma(keV)^2} \cdot \frac{1+2I_e}{1+2I_g} \cdot \frac{1}{1+\alpha_T} \text{ cm}^2$$

where I_e and I_g are the spin numbers for the excited and ground states respectively; E_γ is the resonance energy and α_T is the total internal conversion coefficient. The

natural linewidth has a value of 3.509×10^{-9} keV as given in the Mössbauer Effect Data Index (1958-1965). The experimental linewidth was converted from channels to eV by the following conversion:

$$W \text{ (channels)} \times \frac{\text{Velocity (cm/sec)}}{\text{channel}} \times \frac{E_o \text{ (eV)}}{c \text{ (cm/sec)}}$$

With the data from Table 1, such a graph was plotted (See Fig. 13) and the value of slope obtained was 0.0596. This value yielded a value of 22.1% for the recoilless fraction. The experimental estimate of the natural linewidth found from the graph when extrapolated to zero thickness was 8.07×10^{-9} keV.

IV.3 DETERMINATION OF DEBYE TEMPERATURE

Debye's extension of Einstein's work on the vibrational modes of a crystal led to the introduction of a continuum of oscillator frequencies ranging from zero to a maximum frequency ω_o and obeying a distribution function. This led to an improvement between theory and experiment. Such a distribution was derived by assuming the solid to be a homogeneous and isotropic medium, the group velocity of waves of all frequencies to be the same and the total number of linear oscillators to be equal to three times the

SAMPLE	FWHM (channels)	LINE POSITION (channels)	ABSORBER THICKNESS (inches)	ABSORBER WEIGHT (grams)	ABSORBER RADIUS (centimeters)
$TbVO_{4(1)}$	46.8	126.3	23/1000	0.4112	0.9525
$TbVO_{4(2)}$	45.6	124.3	11/1000	0.2349	0.9525
TbH_3	72.3	128.7	13/1000	0.4372	0.71
$Tb_{(1)}$	108.1	117.3	20/1000	0.5621	0.71
$Tb_{(2)}$	82.9	130.9	11/1000	0.3535	0.71
Tb(3)	58.2	122.6	5/1000 (foil)	foil	0.71

TABLE 1 EXPERIMENTAL OBSERVATIONS

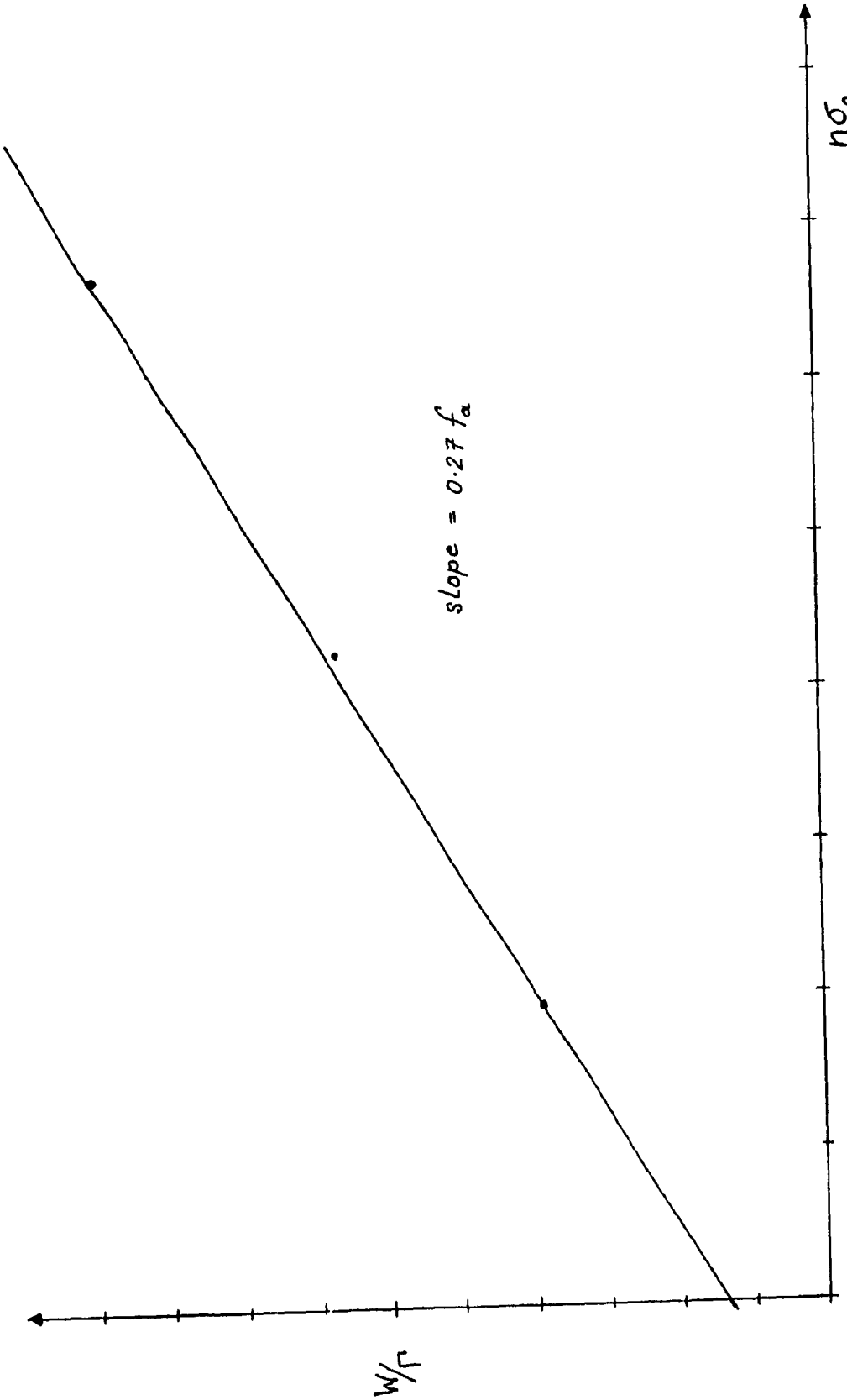

FIG. 13 GRAPH OF W/Γ VS. $n\sigma_o$ USED TO DETERMINE RECOILLESS FRACTION

number N of atoms in a solid. An improvement to Debye's theory, especially at higher frequencies was later pointed out by Born and von Karman.[21]

It is often assumed, for simplicity, that the Debye model is correct and then a characteristic temperature, called the Debye Temperature, θ_D, is defined by the equation:

$$E_D = \hbar \omega_D = k \theta_D \qquad (40)$$

Here ω_D is the cut-off frequency, which, in the Debye theory, is given by the condition that the total number of all oscillators be equal to 3N.

Experimentally, the Debye temperature can be determined from specific heat measurements, from X-ray reflection, from elastic constants, or, as in our case, from the Debye-Waller factor.

The general expression for the Debye-Waller factor is:

$$f_a = \exp\left\{-\frac{6E_R}{k\theta_D}\left[\frac{1}{4} + \left(\frac{T}{\theta_D}\right)^2 \int_0^{\theta_D/T} \frac{x\,dx}{e^x - 1}\right]\right\} \qquad (41)$$

where f_a is the recoilless fraction; E_R is the recoil energy of the emitting or absorbing atom; k is Boltzmann's constant (1.381×10^{-16} ergs/$^\circ$K) and θ_D is the Debye temperature. If the recoil fraction has been determined from experimental

results (as it has in this case), then everything in equation 41 is known, except Θ_D, which may then be determined.

The first step was to rewrite equation 41 as:

$$-\frac{(\ln f_a)k}{6E_R} = \frac{1}{\Theta_D}\left\{\frac{1}{4} + \left(\frac{T}{\Theta_D}\right)^2 \int_0^{\Theta_D/T} \frac{x\,dx}{e^{x-1}}\right\} \qquad (42)$$

and to perform the integration using the following series expansion:[22]

$$\frac{x}{e^{x-1}} = 1 - \frac{x}{2} + \frac{B_1 x^2}{2!} - \frac{B_2 x^4}{4!} + \frac{B_3 x^6}{6!} \quad \cdots (43)$$

where B_i are the Bernoulli numbers. The final result yielded:

$$\Theta_D = \sqrt{\frac{T}{\frac{-(\ln f)k}{6E_R} - \frac{1}{36T}}} \qquad (44)$$

where $E_R = E_o^2/(2Mc^2) = 1.136 \times 10^{-2}$ eV, E_o being the 58.0 keV energy of the transition under study and M being 158.9 amu, the atomic mass of terbium.

The final calculated value of Θ_D for terbium metal was 226.3°K, which is in good agreement with the Debye tempera-

ture of other rare earth elements.

In the limit of either high or low temperature, equation 41 may be rewritten as:

$$\left(f_a\right)_{T\to 0} = \exp\left(\frac{-\frac{3}{2}E_R}{k\theta}\right) \tag{45}$$

$$\left(f_a\right)_{T\to \infty} = \exp\left(\frac{-6E_R T}{k\theta^2}\right) \tag{46}$$

IV.4 INTERPRETATION OF RESULTS

Tb^{159m} decays by gamma emission (58.0 keV, $5/2^+ \longrightarrow 3/2^+$) to Tb^{159}, which is 100% naturally abundant. The ground state of Tb^{159} is probably a [411] Nilsson state with spin and parity $3/2^+$. The 53.0 keV line is the first rotational level of the ground state configuration, its spin and parity being $5/2^+$. The half-life of this transition has been measured by delayed coincidence techniques to be $(1.3 \pm 0.4) \times 10^{-10}$ seconds.[23] The isomeric state of Tb is populated by beta decay from Dy^{159}.

The absorbers were all made by grinding them into the finest possible powder and then simply pressuring them into a small saucer-like disk. In order to conserve the amount of absorber material, prevent cracking at low temperatures, and make weighing the absorber after the experiment possible, no adhesive was used to hold the absorber more firmly in the sample holder. As the whole process was strictly a manual one, obtaining accurate measurements of absorber thicknesses was impossible. The only accurate measurement was the sample's weight.

As the ground state nuclear magnetic moment of Tb^{159} is 1.52 nm, the Tb metal sample should have displayed magnetic hyperfine structure over a $\pm$ 10 cm/sec range.

The most crucial part of the apparatus was the gamma ray detector which had to assist the accompanying electronics in discriminating against the abundant X-radiation. As can be seen from Fig. 4, there existed two intense X-ray peaks (at 44 keV and 50 keV) in the close proximity of the 58 keV peak under study. In order to mask the effect of these two peaks, copper plates two millimeters thick were placed in front of the source. (These absorb the X-rays to a much greater extent than the 58 keV gamma rays).

The Mössbauer resonance obtained with a Dy^{159} (Dy_2O_3) source and Tb metal absorbers of thicknesses 20/1000,

11/1000 and 5/1000 of an inch are shown in Fig. 14, 15 and 16, respectively. Both source and absorbers were maintained at a constant temperature of 80°K. Tb metal is anti-ferromagnetic between 229°K and 221°K and ferromagnetic below 221°K. The observed linewidths were 4.51×10^{-5} eV, 3.46×10^{-5} eV and 2.42×10^{-5} eV, respectively. The per cent resonances in all three case was about 1.4%. The linewidth for this system extrapolated to zero absorber thickness was 8.07×10^{-9} keV, corresponding to a half-life (assuming centred single emission and absorption lines) of 5.65×10^{-11} seconds, in reasonable agreement and comparable accuracy with the measurement by delayed coincidence of $(1.3 \pm 0.4) \times 10^{-10}$ seconds.

Due to the method of absorber preparation, it would be inaccurate to take seriously any of the isomer shifts observed in the spectra for the purposes of calibration.

Unfortunately, there is no resolution of hyperfine lines so that no conclusions can be drawn about the magnetic interactions in Tb metal from this data.

The linewidths observed both by Mössbauer spectroscopy and delay coincidence methods in Tb^{159} have energy widths which must be considered wide (by Mössbauer spectroscopy standards).

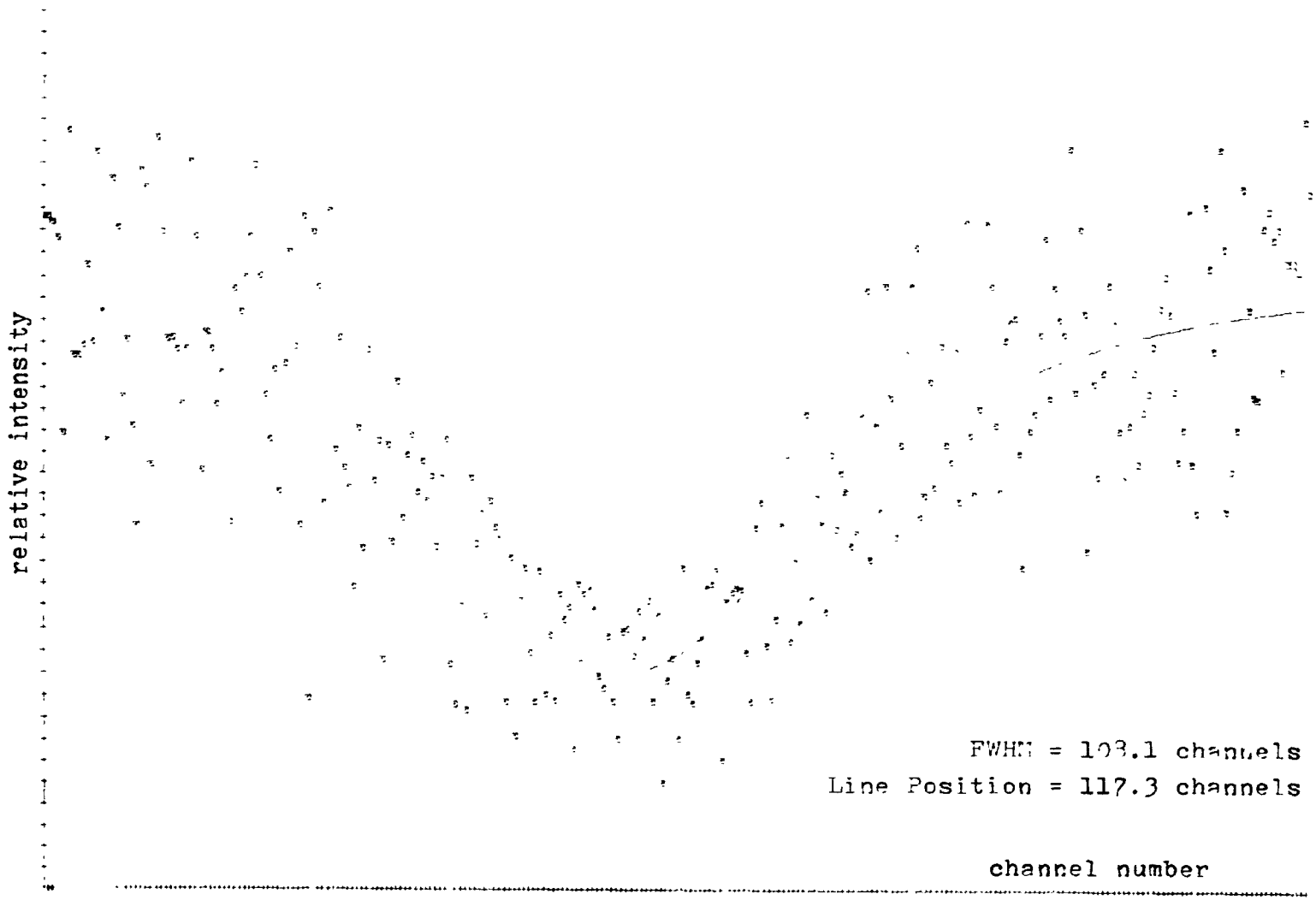

Fig. 14 Mössbauer Spectrum of Tb Metal (Thickness = 20/1000 inch).

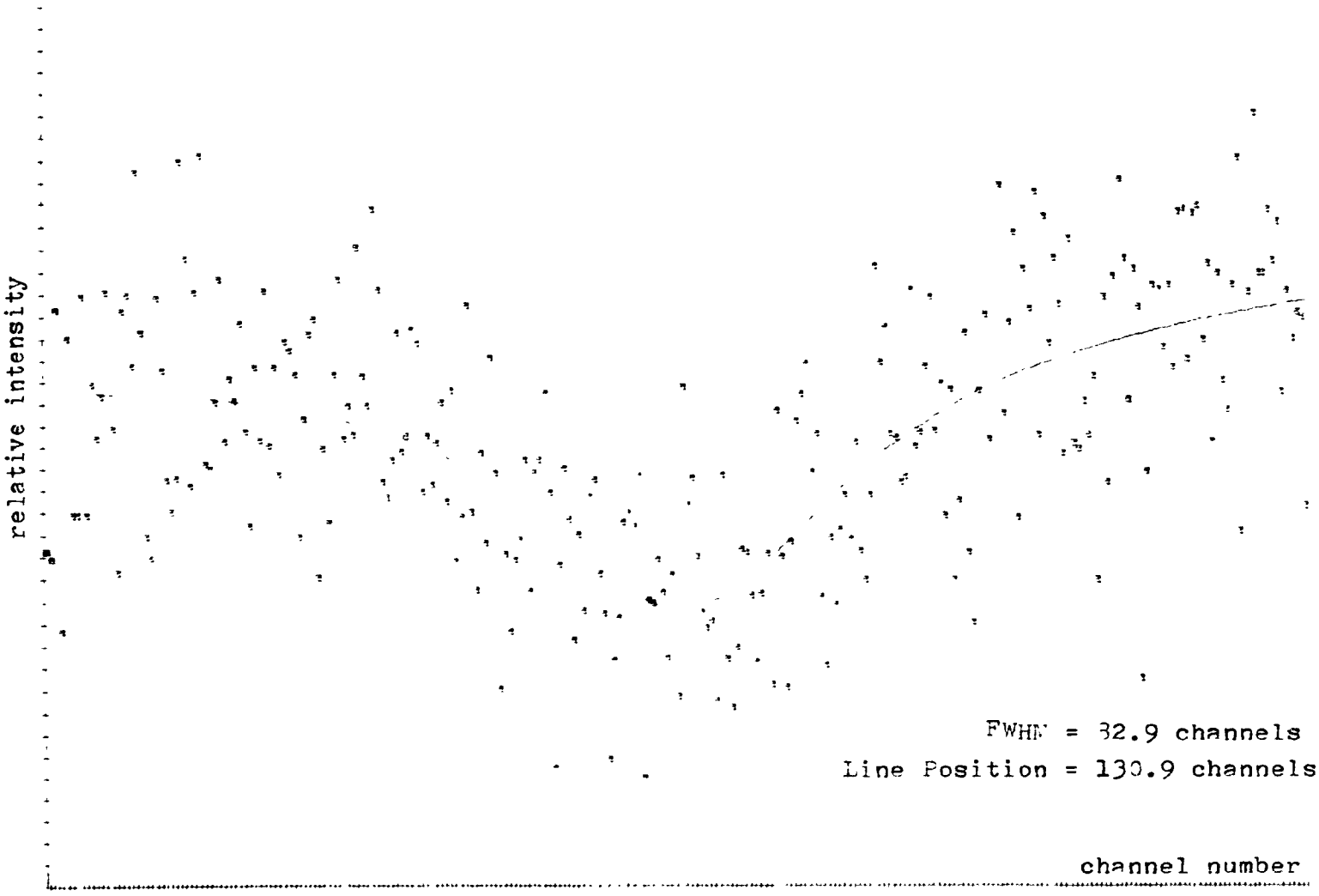

Fig. 15 Mössbauer Spectrum of Pb Metal (Thickness = 11/1000 inch).

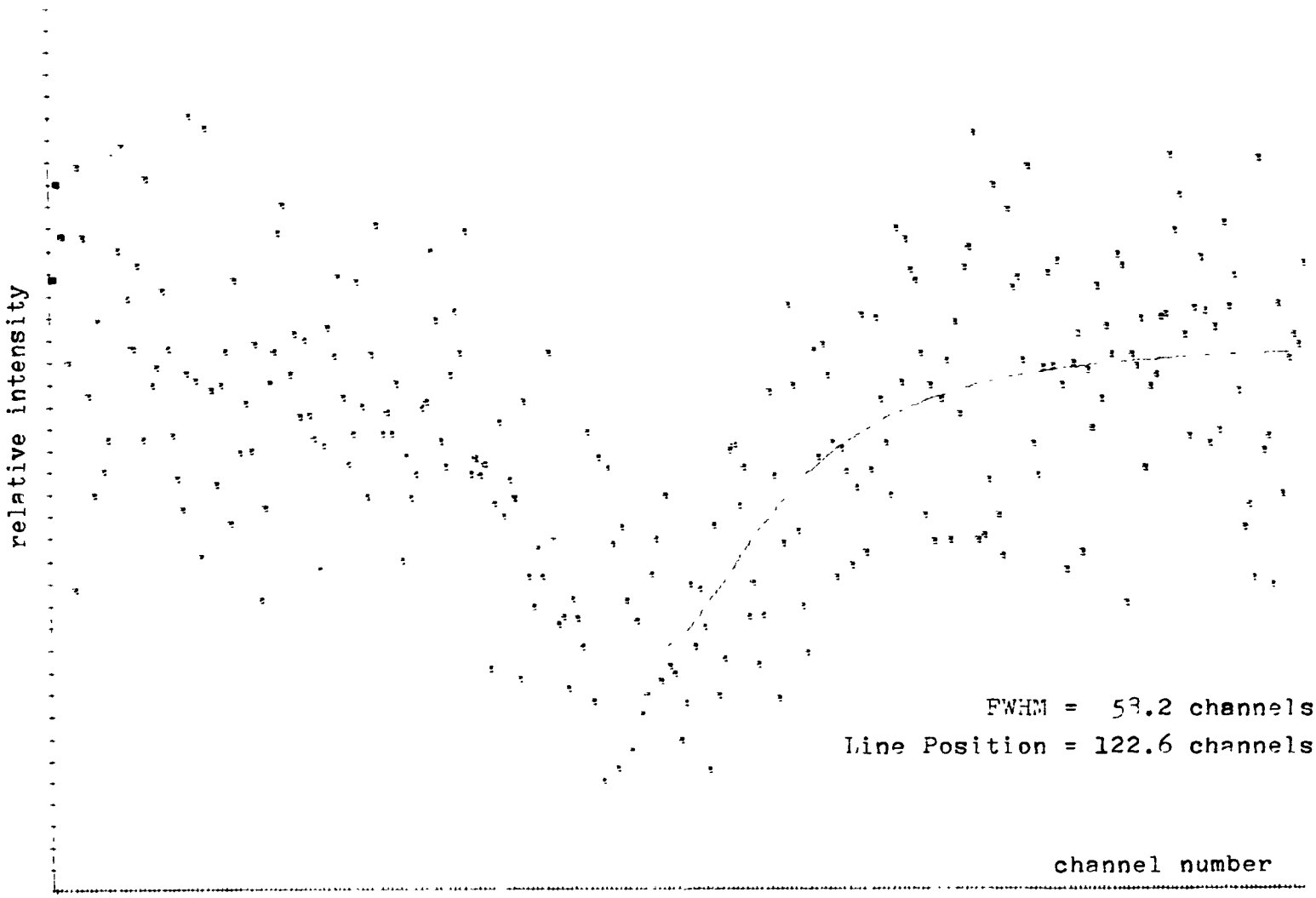

Fig. 16 Mossbauer Spectrum of Tb Metal (Thickness = 5/1000 inch).

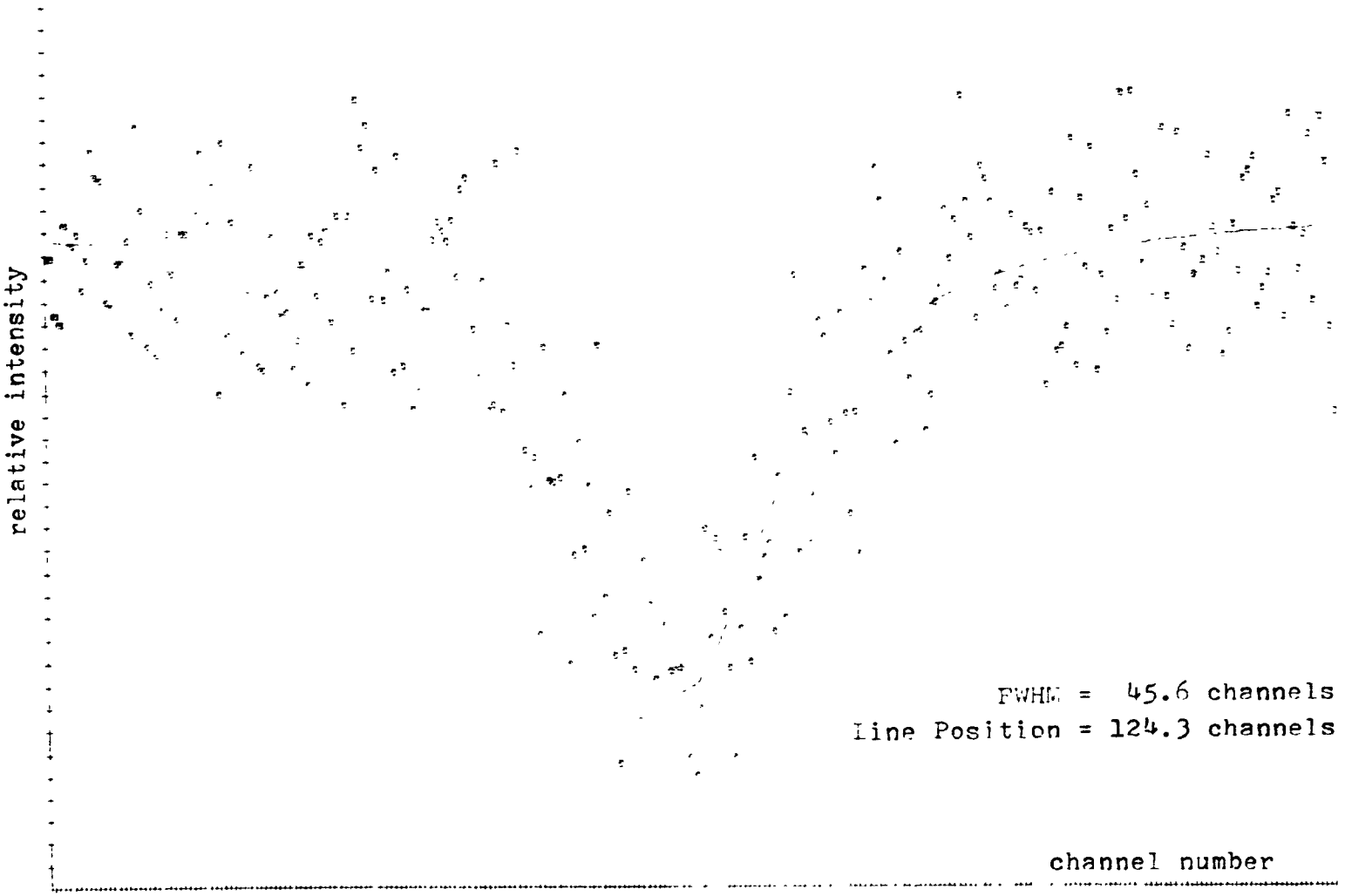

Fig. 17 Mössbauer Spectrum of $TbVO_4$.

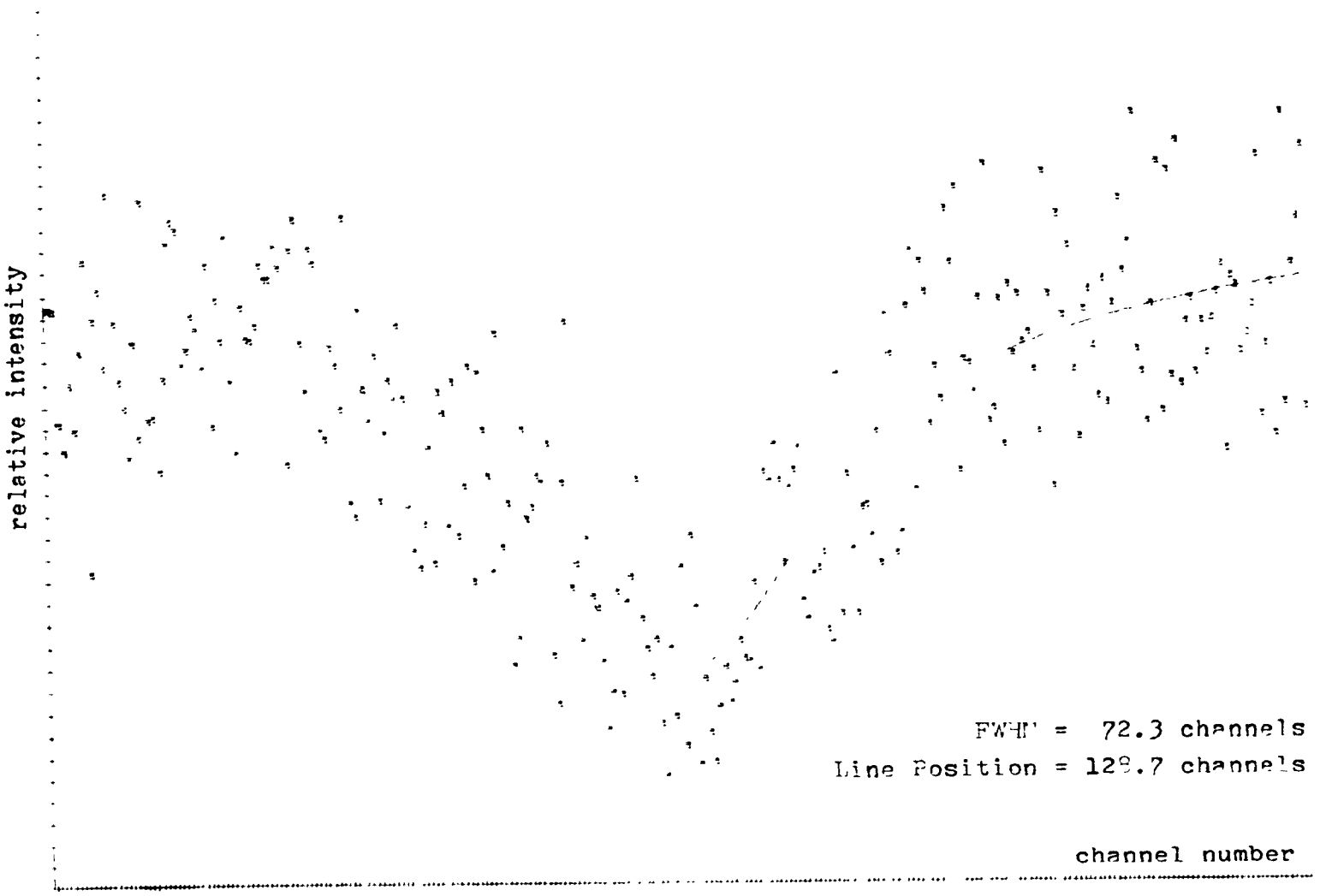

Fig. 18 Mössbauer Spectrum of TbH_3.

V. CONCLUSIONS

The experiments performed in the preparation of this paper required a good basic knowledge of the instrumentation required in nuclear physics, and an understanding of Mössbauer spectroscopy techniques. They also served to illustrate many of the difficulties encountered in trying to obtain precise narrow absorption peaks.

The linewidths of all the spectra observed were larger than twice the natural linewidth (i.e., 3.509×10^{-9} keV) for terbium metal. The natural linewidth being the most accurate possible determination for the energy difference existing between the two states in question. This increase in linewidth indicated that the Mössbauer lines were being broadened by some external perturbation or by some factor inherent in the experimental set-up. The most important factor leading to this line broadening was the preparation of the powder and granular sources. This topic (distortion due to source preparation) has received its first detailed discussion by Bowman et. al.[24] Another factor that may also have played its part in distorting the spectrum was disturbance from vibrations, particularly those resulting from the presence of a vacuum pump working in close proximity to the Mössbauer equipment throughout the course of the experiments.

The linewidth of Tb metal extrapolated to zero absorber thickness was 8.07×10^{-9} keV corresponding to a half-life of 5.66×10^{-11} sec. Mössbauer resonances were also obtained with Dy^{159} - $TbVO_4$ and Dy^{159} - TbH_3 combinations. These resulted in observed linewidths of 1.91×10^{-8} keV and 3.02×10^{-8} keV respectively. (See Fig. 17 and 18). The linewidths yielded values of 2.43×10^{-11} sec and 3.04×10^{-11} sec for the half-lives of $TbVO_4$ and TbH_3 respectively. The values of the half-lives obtained were found in reasonable agreement with the value of $1.3 \pm 0.4 \times 10^{-10}$ sec, as measured by delayed coincidence techniques and the value of 9.6×10^{-11} sec obtained by Woolum and Bearden[25] in Mössbauer effect experiments.

As a result of the broadened linewidths, it was impossible to use the area method or the comparison method to determine the recoilless fraction for Tb. The linewidth dependence on absorber thickness was the method chosen, as it dealt only with the ratio of experimental linewidth to natural linewidth, not on the absolute value of the experimental linewidth. This method yielded a value of 22.1%, a result that was in very good agreement with the recoilless fraction of 23%, previously arrived at.[17] As only one experiment was performed using TbH_3 and two with $TbVO_4$, there was not sufficient data available to determine the recoilless fraction by the method of linewidth dependence on

absorber thickness for these two different absorbers.

The determination of the Debye temperature was made possible by the previous evaluation of the recoilless fraction and resulted in the value of 226°K which agreed very closely with the value suggested by Goldanski.[17]

The calculated value of the half-life of Tb was understandably different from previously determined values, which resulted from the fact that the calculation depended solely on the experimental linewidth. It should also be noted that there is a considerable deviation between results obtained for the half-life of Tb using different experimental methods.

All of the experiments ran for at least 72 hours, which proved to be necessary due to very low count rates and a very small per cent resonance, with both source and absorber maintained at 80°K. Even after this time period, the counts were well spread out and much more time would have been required to improve statistics. It is as a result of the poor statistics that no valid conclusions could be drawn concerning the apparent isomer shifts observed in some of the spectra.

It should also be pointed out that Woolum and Bearden[25] as well as Atzmony et. al.[26] have both encountered unusually

large (by Mössbauer spectroscopy standards) experimental linewidths for Tb and its compounds. The reasons for this are still very much in question.

BIBLIOGRAPHY

1) W. Kuhn, Phil. Mag., 8, 625 (1929).

2) P.B. Moon, Proc. Phys. Soc., 63, 1189 (1929).

3) R.L. Mössbauer, Z. Physik, 151, 124 (1958).

4) W.E. Lamb, Jr., Phys. Rev., 55, 190 (1939).

5) J.D. Jackson, Can. J. Phys., 33, 575 (1955).

6) H. Lustig, Am. J. Phys., 29, 34 (1961).

7) R.L. Mössbauer and D.H. Sharp, Rev. Mod. Phys., 36, 410 (1964).

8) G.K. Wertheim, Mössbauer Effect: Principles and Applications, Academic Press, New York (1964).

9) E. Fermi and E. Segre, Z. Physik, 82, 729 (1933).

10) J. Heberle, Nuclear Instr. Methods, 58, 90 (1968).

11) W.M. Visscher, (unpublished notes), Los Alamos Scientific Laboratory.

12) D.A. O'Connor, Nuclear Instr. Methods, 21, 318 (1963).

13) D.A. Shirley and M. Kaplan, Nuclear Instr. Methods, 123, 816 (1963).

14) G. Lang, Nuclear Instr. Methods, 24, 425 (1963).

15) D.W. Hafemiester and E.B. Shera, Nuclear Instr. Methods, 41, 133 (1966).

16) R.L. Mössbauer and W. Wiedermann, Z. Physik, 159, 33 (1960).

17) V.I. Goldanski and R.H. Herber, Chemical Applications of Mössbauer Spectroscopy, Academic Press, New York (1968).

18) K. Nozik and M. Kaplan, Phys. Rev., 159, 273 (1967).

19) A.C. Melissinos, Experiments in Modern Physics, Academic Press, New York (1966).

20) H.D. Young, Statistical Treatment of Experimental Data, McGraw Hill Book Co., (1962).

21) M. Born and Th. von Karman, Z. Physik, 13, 297 (1912).

22) H.B. Dwight, Tables of Integrals, The MacMillan Co., New York (1961).

23) E.E. Berlovich, N.P. Bonetz and V.V. Nikitin, Bull. Acad. Sci. USSR Phys., 25, 210 (1961).

24) J.D. Bowman, E. Kankeleit, K.W. Kaufman and B. Persson, Nuclear Instr. Methods, 50, 13 (1967).

25) J.C. Woolum and A.J. Bearden, Phys. Rev., 142, 143 (1966).

26) U. Atzmony, E.R. Bauminger and S. Offer, Nuclear Phys., 89, 433 (1966).